Mineral Res. Expl. Bull., 120, 1-35,1998

# AN APPROACH TO THE ORIGIN OF KESİKKÖPRÜ (BALA-ANKARA) IRON DEPOSIT

Bilgin DOĞAN*; Taner ÜNLÜ** and İ. Sönmez SAYILI**

ABSTRACT.- This study discusses the ore geology and origin of the Kesikköprü (Bala- Ankara) iron deposit. The basement composed of gneiss, schist, and quartzites of Paleozoic- Mesozoic Kırşehir massive is overlain by sedimentary and volcanic-volcaniclastic rocks that consist of spilitic basalt, basaltic tuff, diabase dikes, cherty limestone, radiolarite, and mudstone-limestone lenses which are transitional with an ophiolitic melange made of crystallized limestone blocks and ultramafic-mafic rocks in a basin that was formed during the upper Cretaceous time. Rocks of the basin are cut by granitoids such as granite, granodiorite, and porphyries of Maastrichtian-Paleocene age. These units are unconformably covered by Eocene Çayraz formation consisting of sandy, clayey, fosiliferous limestone, Miocene-Pliocene (?) İncik formation composing of siltstone, claystone, anhydrite-gypsum alternations, and sandstones with limestone and fosiliferous limestone blocks, volcanic rocks made of rhyolite and tuffs, Pliocene-Quaternary Kızılırmak formation consisting of gravel, sand and mud deposits, and finally post-tectonic basin sediments of Quaternary alluvium. Possible lithologies for source and country rocks of mineralization are examined under two main groups as ultramafic rocks consisting of crystallized limestone blocks, peridotite, pyroxenite, and serpentinites and mafic rocks consisting of gabbro and diabases while in more detail, they are investigated as serpentinites and mafic rocks subjected to hydrothermal alteration. The association among olivine, pyroxene, and plagioclase minerals is distinctive in field, thin section, and XRD studies. Petrographic works conducted on mafic and ultramafic rocks yield occurrences unique to ultramafic cumulates. Ore samples, in the order of abundance, consist mainly of magnetite and lesser amounts of pyrite, chalcopyrite, chromite, siderite, ankerite, and trace amounts of pentlandite, pyrrhotite, gersdorffite, ilmenite, and sphene. In addition, olivine, pyroxene, tremolite, and actinolite also accompany the ore and calcite and dolomite are also observed in crack and fracture fillings. Geochemical studies performed on the ore samples indicate that granitic fluids have no direct effect in the ore formation. The processes of granitic intrusions associated with hydrothermal convection cell affect the mafic rocks and shape the hydrothermal alteration modes formed by "skarn type minerals" and fels-like textures". Expelling of iron element as a result of serpentinization of ferromagnesian minerals within the ultramafic rocks, such as olivine and pyroxene, is the primary source of iron. Their secondary enrichment by the granitic intrusions indicates another important stage in the formation of Kesikköprü iron deposit. Present study favors the idea that Kesikköprü iron deposit is similar to the Divriği type deposit, in other words, as also stated by previous works, iron was derived directly from the granitic rocks.

## INTRODUCTION

This study discusses the formation of Kesikköprü (Bala-Ankara) iron deposit located in the Bala town of the city of Ankara designated in Kırşehir J30 b-3 quadrangle.

The basement in the vicinity of study area comprised by rock assemblages of Kırşehir massive is overlain by the upper Cretaceous ophiolitic complex together with sedimentary and volcanic-volcaniclastic rocks and by a sedimentary cover of Tertiary age.

Some of studies on the lithostratigraphy of the Kırşehir massive and its vicinity are of Ketin (1963), Norman (1972), Çapan and Buket (1975), Göncüoğlu (1977), Tülümen (1980), Erkan (1981), Erkan and Ataman (1981), Seymen (1982), Bayhan (1986), Önen and Ünan (1988), Erler et al., (1989-1991), and Erler and Bayhan (1995) while some of studies on tectonics are of Bailey and Mc Callien (1950), Egeran and Lahn (1951), Ketin (1955), Seymen (1982), and Akıman et al., (1993). The main studies on the general geology and ore geology of the Kesikköprü area are of Brennich (1960), Kraeff (1962), Boroviczeny (1964a, *b, c, d),* Yaz and Sözen (1965, 1967), Sözen (1970), Sungurlu (1970), Öztürk et al., (1983), Öztürk and Öztürk (1983), Bayhan (1984), Bilgin et al., (1986), Kara and Dönmez (1990), and Wondemagegnehu (1990).

Iron deposits in the Kesikköprü area have been worked since 1960's. However, the studies could not go in detail on the origin of the ore. Although there are no sufficient information on the origin, considering the its close relation to the crystallized limestones, the idea that mineralization is a metasomatic type was widely

accepted by most of the workers while the type of the country rock is still controversial among the workers. Some of the authors suggest that rocks associated with the mineralization are basic in composition while some set forth granitic rocks and propose a skarn type mineralization with an epigenetic character formed as a result of interaction between limestones and iron-rich solutions derived from granitic rocks.

Source of iron element in the Kesikköprü iron deposit is the fatal importance of the controversy on the origin of mineralization. It is the aim of present study to introduce a new aspect to such controversy.

## GEOLOGY OF THE STUDY AREA

Geology of five different fields covering an area of about 225 $km^2$ was revised on 1/25.000 scaled geology maps (Fig. 1). Studies in the field no. I were directed to intense sampling and revision of geological maps while works in other fields were carried out by sampling and revision of geological maps based on the setting of stratigraphy. Geology of the areas out of the study fields was taken from the studies of Bilgin et al., (1986) and Dönmez (1990). Field no. I in which Kesikköprü iron deposit is located comprises 100 $km^2$ part of the Kırşehir J 30 b1, b2, b3, and b4 quadrangles (Fig. 2).

Within the ophiolitic complex exposing around the study area, are the sedimentary and volcanic-volcaniclastic rocks being transitional with the melange, crystallized limestones, and ultramafic-mafic rocks, all intruded by granitoids and blanketed by a sedimentary cover alternated with volcanic fragments. A total of 300 thin sections was prepared, 250 samples from above mentioned lithologies and 50 from pit samples, for mineralogic-petrographic examinations. In addition, a number of 50 samples was subjected to XRD studies. The results are summarized as follow.

### Crystallized limestones

Crystallized limestones are exposed in Kartalkaya ridge and arotind Bolkardağı northeast of field no. I and in a narrow part of field no. II to the northwest and northeast and southeast sections of field no. V.

Crystallized limestones are composed of gray, yellowish beige, white colored, fractured, thick bedded, sugar-textured, coarsely crystalline carbonaceous rocks alternated with dolomitic levels comprising the topographic heights with no vegetation cover.

Petrographic examinations reveal the presence of medium-coarse to very coarse grained, equigranular recyrstallized calcites also showing sutured pressure twinnings accompanied by fine to medium grained, partly euhedral dolomite occurrences.

Crystallized limestones in the area are observed as blocks within the upper Cretaceous ultramafic-mafic rocks and unconformably covered by Pliocene-Quaternary sedimentary rocks. They are intruded by granitic rocks giving rise to formation of skarn occurrences at the contacts.

The age of crystallized limestones, in a broad range, is suggested to be Paleozoic-Mesozoic by previous workers (Öztürk et al., 1983; Bilgin et al., 1986; Kara and Dönmez, 1990).

### Ultramafic-mafic rocks

Ultramafic-mafic rocks are exposed south of Kesikköprü plateau, around Bolkardağı and southeast of Kartalkaya ridge in the field no. I, in between Kalemkamış hill at northwest and Uzunmezarın hill mideast of the field no. II, and central parts of the field no. III along an east-west direction.

Ultramafic-mafic rocks in the field no. I are gray, light gray, greenish, and earth brown colored and composed of pyroxenite, gabbro, and diorite type rocks that are detected to be altered where the color gets lighter while those of field no. II are dark gray, green colored, densely fractured and consist of serpentinite, peridotite, pyroxenite, and gabbro-diorite type rocks with a magnetic susceptibility even determined by a hand magnet. Ultramafic-mafic rocks in the field no. III are light green, green, dark green and black colored, densely fractured and fissured. Magnetic susceptibility is distinctive in places. They comprise serpentinite, peridotite, and pyroxenite around the Set hill while they consist of peridotite and gabbroic type rocks in the vi-

cinity of Hirfanlı dam axle, Karapınar Beli hill, and Hirfanlar village. Ultramafic-mafic rocks are cut by granitic rocks and fractured and subjected to the hydrothermal alteration.

As a result of petrographic examinations, ultramafic rocks are grouped as peridotites (intensely alteration of serpentinites to dunite and lherzolite), pyroxenites (clinopyroxenite, olivine, and websterite), and serpentinites while mafic rocks are grouped as mafic plutonic rocks (gabbro and diorite) and mafic sub-plutonic rocks (diabase and diorite porphyry).

Since it is intruded by granitic rocks, the basement of ultramafic-mafic rocks cannot be observed in the study area. Studies conducted out of the area indicate that the contact between lithologies unique to metamorphic basement of the Kırşehir massive and ultramafic-mafic rocks is tectonic one (Seymen, 1982). The upper contact of ultramafic-mafic rocks in the area is covered with young terrestrial deposits while that out of the study area is blanketed by marine sediments (Bilgin et al., 1986; Kara and Dönmez, 1990).

According to Seymen (1982) and Bayhan (1986), the age of ultramafic-mafic rocks is Jurassic-Campanian while Bilgin et al., (1986) and Kara and Dönmez (1990) suggest upper Cretaceous and Cenomanian-Santonian (?) ages, respectively, for the unit.

Ultramafic-mafic rocks seem to be correlated with the Ankara melange (Bailey and Mc Callien, 1950).

### Sedimentary and volcanic-volcaniclastic rocks

Volcanosedimentary rocks in the field no. IV are widely exposed in the area between P6hrenk, Yenimerdan, Efendiköy, and Kasımağa villages while they are cropped out Salik hill, west of Deve hill, and around the Halildede in the field no. V.

Sedimentary and volcanic-volcaniclastic rocks appear in beige, white, gray, light gray, greenish, and earth brown colors. In some places, due to the effect of iron-rich fluids and oxidation, red color becomes dominant. Sedimentary rocks with volcanic intercalations show a regular sequence. The unit appears to be a volcanosedimentary assemblage consisting of spilitic basalt, basaltic tuff, diabase dikes, cherty limestones, radiolarite and mudstone-limestone band and lenses.

As a result of petrographic examinations, sedimentary and volcanic-volcaniclastic rocks are grouped as basalt, spilitic basalt, radiolarite and pelagic limestone.

Its basement cannot be observed in the area. They are cut by granitic rocks and unconformably covered with young volcanic and sedimentary rocks.

Bilgin et al., (1986) were named the unit as the Kasımağa formation with an age of upper Cretaceous and suggested that Kasımağa village is the type location.

### Granitic, rocks

Granitic rocks are found around the Kesikköprü town, east of the Kesikköprü plateau, around the Camiisagir village and Maden hill in the field no. I, north, south, and east of the field no. II, around the Tavşancıl hill north-northeastern part of the field no. III and Ziyaret hill at southwest, and finally northeastern section of the field no. V.

They comprise high elevations and rugged terrains in the area. They appear as fractured and fissured and in white, gray, pink gray, and red colors. In hand samples, they are medium grained and display dark and light color tones but mostly dominated by pink and gray colors. It is partly disintegrated and subjected to arenitization.

As a result of petrographic examinations, granitic rocks are combined into three groups as granite, granodiorite, and granodiorite porphyry which show a compositional change in a narrow range.

Granitic rocks are intruded into crystallized limestones and ultramafic-mafic rock's and intensely altered them. They are unconformably overlain by marine and terrestrial sedimentary rocks of Eocene and Pliocene-Quaternary age.

Considering the radiometric determinations, the ages of some granitic rocks exposing in the region are

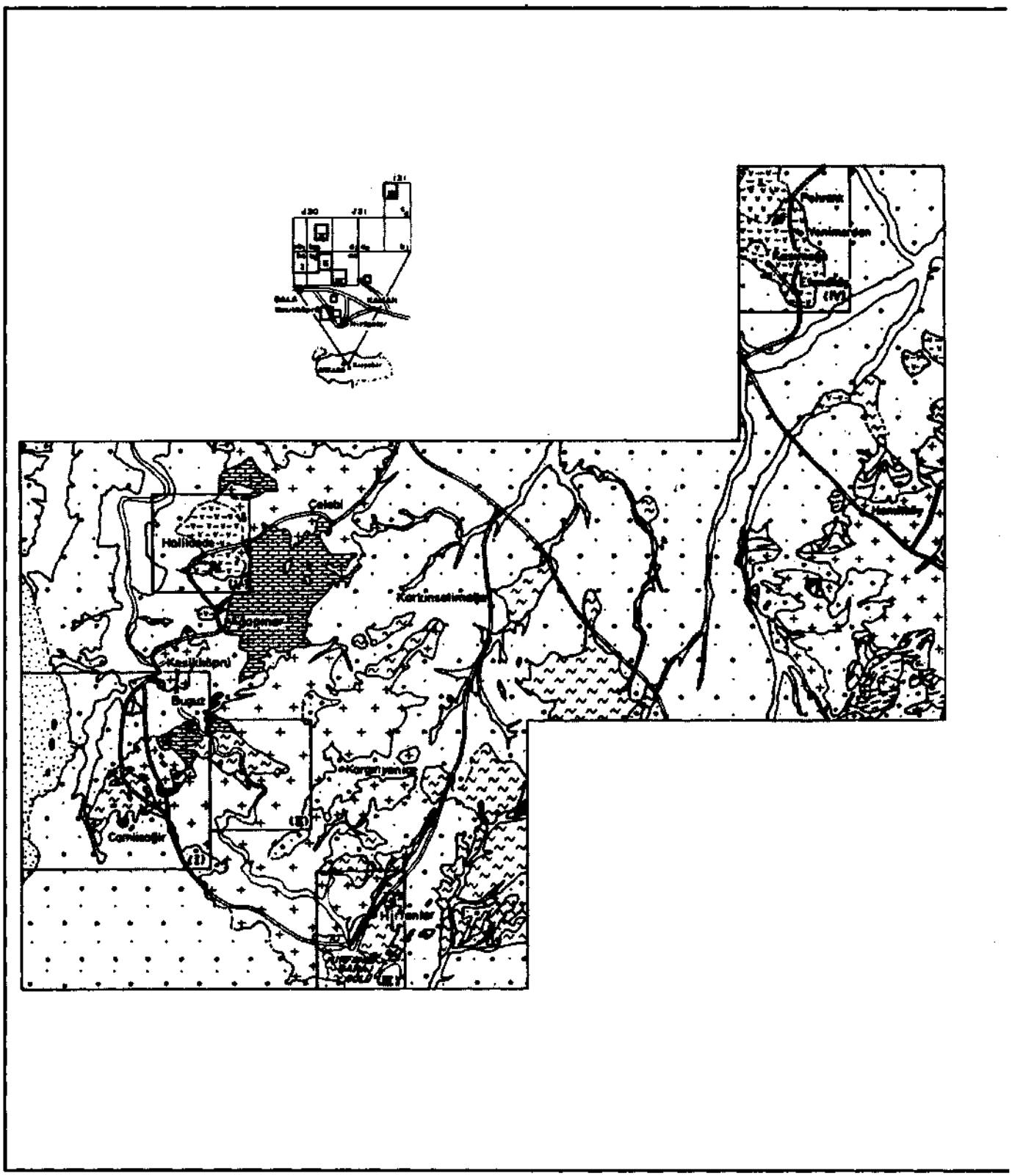


Fig. 1- Geological map of Kesikköprü and surroundings. Fields nos I, II, III, IV and V represent the studied areas (Modified from Doğan, 1996).

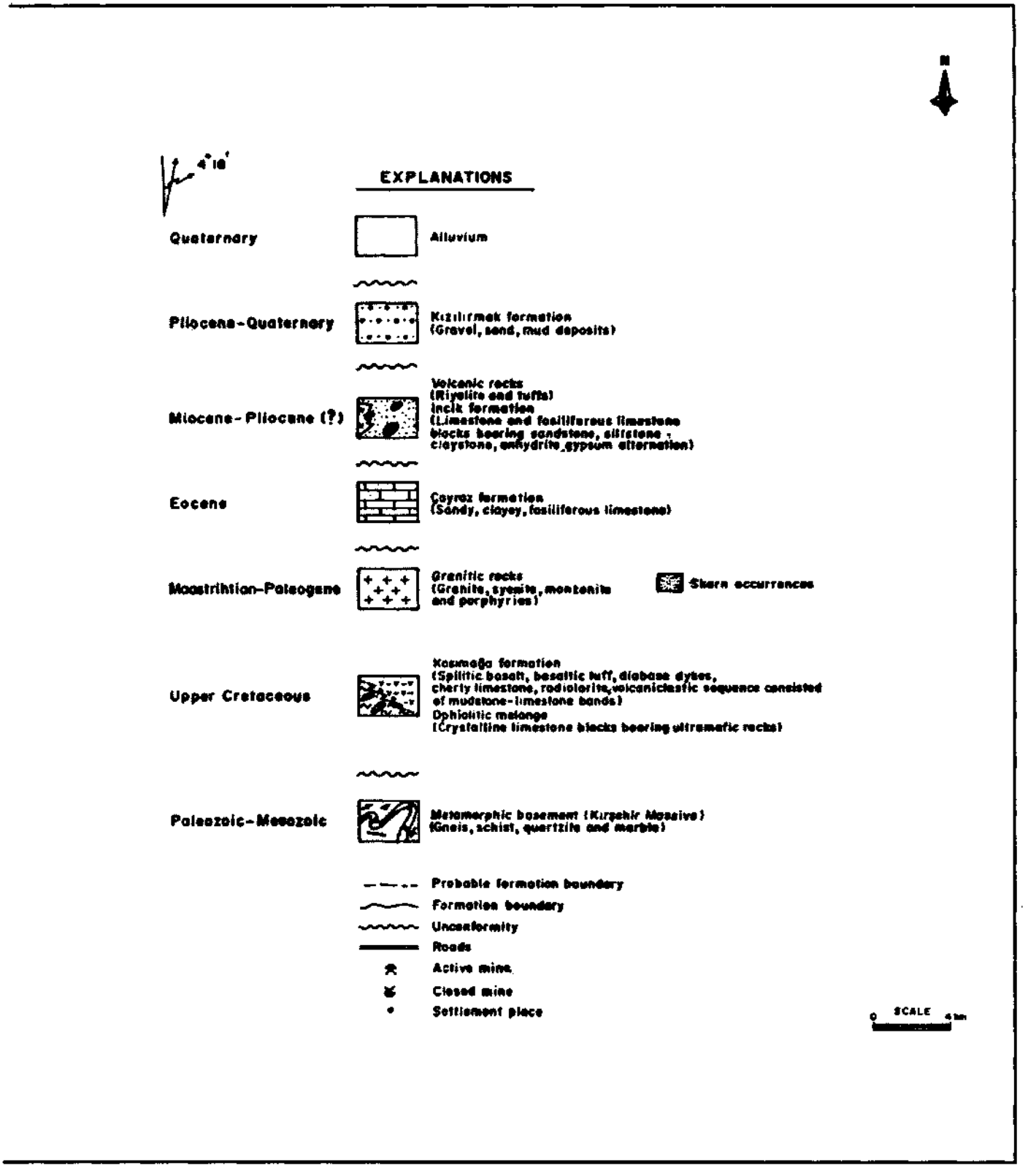
N
EXPLANATIONS
Quaternary
Alluvium
Pliocene-Quaternary
Kızılırmak formation
(Gravel, sand, mud deposits)
Miocene-Pliocene (?)
Volcanic rocks
(Rhyolite and tuffs)
Incik formation
(Limestone and fossiliferous limestone
blocks bearing sandstone, siltstone ,
claystone, anhydrite gypsum alternation)
Eocene
Çayraz formation
(Sandy, clayey, fossiliferous limestone)
Maastrihtian-Paleogene
Granitic rocks
(Granite, syenite, monzonite
and porphyries)
Skarn occurrences
Upper Cretaceous
Kasmağa formation
(Spilitic basalt, basaltic tuff, diabase dykes,
cherty limestone, radiolorite, volcaniclastic sequence consisted
of mudstone-limestone bands)
Ophiolitic melange
(Crystalline limestone blocks bearing ultramafic rocks)
Paleozoic-Mesozoic
Metamorphic basement (Kırşehir Massive)
(Gneis, schist, quartzite and marble)
Probable formation boundary
Formation boundary
Unconformity
Roads
Active mine
Closed mine
Settlement place
0 SCALE 4 km

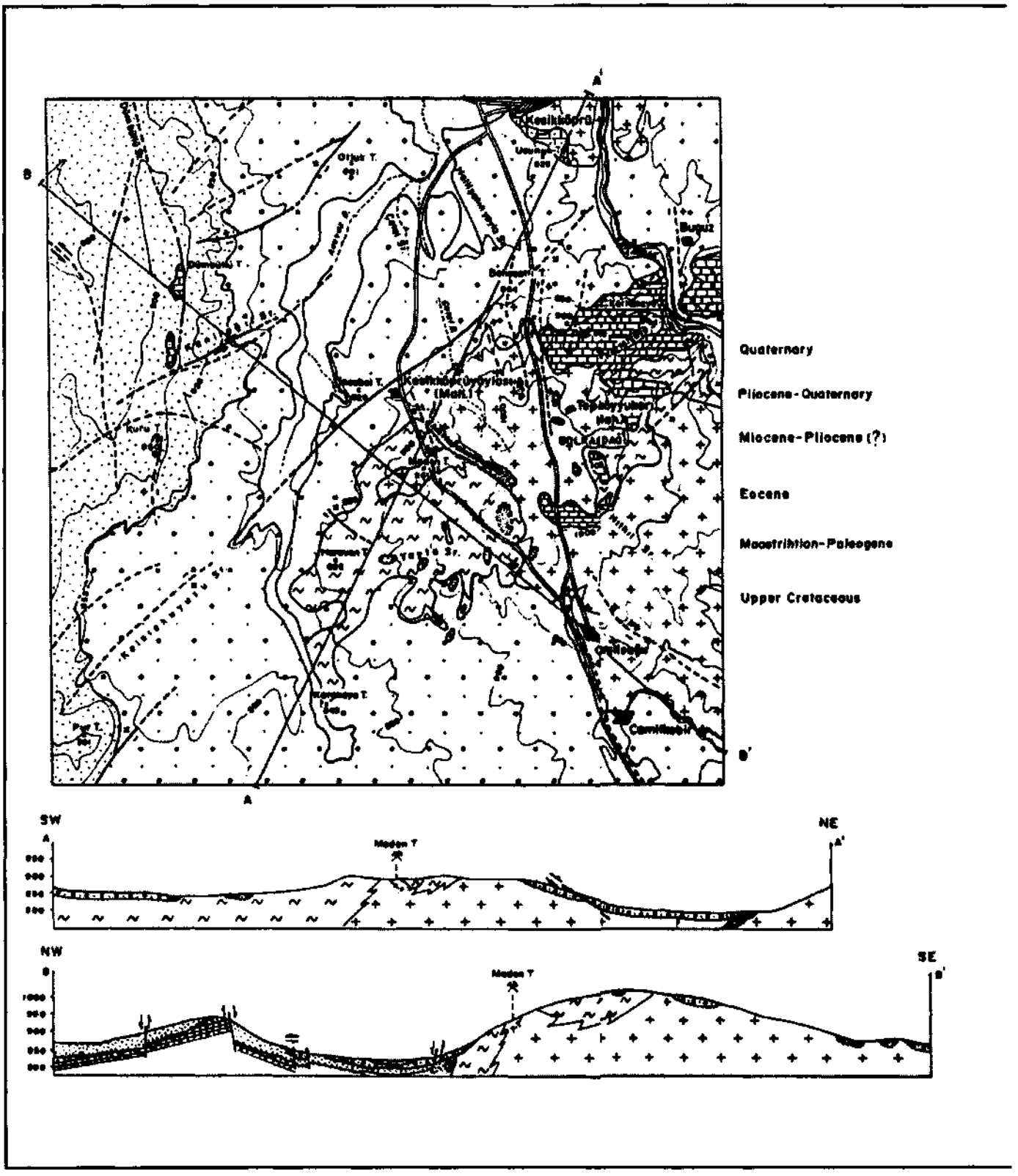


Fig. 2- Geogical map of Field no I at Kesikköprü iron deposit (Modified from Doğan, 1996).

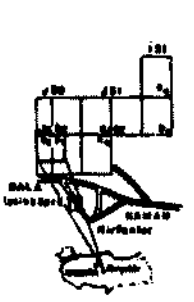

N

**EXPLANATIONS**

- Alluvium
- Kızılırmak formation (Gravel, sand, mud deposits)
- İncik formation (Limestone and fossiliferous limestone blocks bearing sandstone, siltstone, claystone, anhydrite-gypsum alternation)
- Çayraz formation (Sandy, clayey fossiliferous limestone)
- Kesikköprü granitoid (Granite, granodiorite and porphyries)
- Skarn occurrences
- Ophiolitic melange (Crystalline limestone blocks bearing ultramafic rocks
- Probable formation boundary
- Formation boundary
- Fault probable
- Fault
- Unconformity
- Counteur
- A — A' Cross-section line
- Roads
- Active mine
- Projected ore boundary
- Settlement place
- Closed mine

0 SCALE 1 km

proposed to be 54 Ma-Eocene (Ayan, 1963), 71 Ma-upper Cretaceous (Ataman, 1972), and 110 Ma-lower Cretaceous (Güleç, 1994). Based on the observations performed around the study area, different ages were also suggested: Paleocene-Eocene (Öztürk et al., 1983), upper Maastrichtian-Eocene (Bilgin et al., 1986), pre-Maastrichtian or Santonian-Campanian (?) (Kara and Dönmez, 1990). Since granitic rocks are unconformably covered by Eocene units and since they cut the upper Cretaceous units together with consideration of findings of other workers (Bilgin et al., 1986), their age is assigned to be Maastrichtian-Paleocene.

Some of granitic rocks exposing in Central Anatolia are named as Baranadağ massive (Ayan, 1963), Cefalıkdağ granodiorite (Ataman, 1972), Karacaali pluton (Norman, 1972), Üçkapılı granodiorite (Göncüoğlu, 1977), Baranadağ and Buzlukdağ plutons (Seymen, 1982), Çelebi Intrusion (Bayhan, 1986), Ortaköy granitoid (Atabey et al., 1987), and Baranadağ granitoid (Kara and Dönmez, 1990). Since granitic rocks observed in the field no. I have not been named previously and widely exposed around the Kesikköprü town, in the present study, they are called as the Kesikköprü granitoid.

### Skarn occurrences

They are found on the contacts of limestone-granitic rocks in the area between Kartalkaya, Bolkardağı, Maden hill, and Kesikköprü plateau and appear as tightly massive blocks.

As a result of petrographic examinations, fine to medium grained, fels-textured rocks of monomineralic composition were determined, such as epidote-fels, vesuvian-fels, garnet-fels, and diopside-fels consisting of epidote, vesuvian, garnet, and diopside minerals.

### Sedimentary rocks

Sedimentary rocks are exposed in wide areas between Dumbullu ridge and Pur hill at north, south, and western parts of the field no. I, a limited area at northwestern part of the field no. II, around the Hirfanlı dam lake in the field no. III, south and east of the field no. IV, south and west of the field no. V, and outside of the study area.

Sedimentary rocks of the Çayraz, İncik, and Kızılırmak formations are cropped out in the field no. I while sedimentary rocks of only the Kızılırmak formation are exposed in the field nos. II, III, IV, and V.

*Çayraz formation.-* It is exposed in a limited area around the Kesikköprü town in the field no. I.

The unit is composed of reddish beige colored, clayey, sandy, abundantly Nummulites sp.-bearing limestones that are observed as blocks in places.

It unconformably overlies the Kesikköprü granitoid while its upper contact is unconformably overlain by the Kızılırmak formation.

Considering the findings of previous workers (Bilgin et al., 1986), age of the Çayraz formation is accepted to be Eocene.

Lithologies with similar features are also named as Çayraz formation by Schmidt (1960) and Bilgin et al., (1986).

*İncik formation.-* Sedimentary rocks exposing in the area between Dümbüllü ridge and Pur hill west of the field no. I comprise lacustrine and fluvial facies.

Formation is composed of red, beige, and greenish earth brown colored limestone and alternations of sandstone, siltstone, claystone, and anhydrite-gypsum that also contain fosiliferous limestone blocks of upper Cretaceous-Eocene age.

The basement of the İncik formation in the area could not be detected while its upper contact is unconformably overlain by the Kızılırmak formation.

Considering the findings of previous workers (Bilgin et al., 1986), age of the formation is accepted to be Miocene-Pliocene (?).

*Kızılırmak formation.-* It is widely cropped out in the field nos. I, IV, and V while it covers a limited area in the field nos. II and III.

Unit is generally observed in beige, grayish beige, greenish earth brown, and earth brown colors. It characterizes loosely cemented slope molasse and fluvial sediment and composed of gravel, sand, and mud accumulations.

Its lower contact is discordant with the Çayraz and İncik formation while its upper contact is discordant with young alluvium deposits.

Based on field observations and findings of previous workers (Bilgin et al., 1986), age of the Kızılırmak formation is believed to be Pliocene-Quaternary.

### Volcanic rocks

They are exposed in wide areas between Göztepe and Tütün hill northwest of Kasımağa village and abandoned manganese occurrences in the field no. IV. They are observed to comprise high elevations in the area.

Volcanic rocks are generally beige, white, gray, and light gray in color.

Petrographic examinations indicated that volcanic rocks can be grouped as those intensely silicified in narrow areas, carbonaceous in places, and the ones containing high amount of quartz rhyolite-rhyodacite and tuffs.

Volcanites unconformably cover the volcanosedimentary rocks. Based on the previous works conducted in the region (Akyürek et al., 1984), their age is accepted as Miocene.

### Alluvium

It is observed along the Kızılırmak River. They are recent occurrences and composed of the mixture of gravel, sand, silt, and soil comprising the river and valley beds and flat areas. They also contain the material of older units.

It unconformably rests above the Kızılırmak formation and has an age of Quaternary.

## RESULTS OF FIELD WORKS

The findings obtained from the field works are given below:

Crystallized limestones that were included to metamorphic basement in previous studies (Öztürk et al., 1983; Bilgin et al., 1986; Kara and Dönmez, 1990) are evaluated as the limestone blocks within the ophiolitic complex (field nos. I and II).

Ultramafic-mafic rocks and such limestone blocks were mapped together as the ophiolitic complex. Karakaya ultramafite (field no. III) described in the study of Seymen (1982) is included to the ophiolitic complex.

Lithologies of field no. I that were included to the Kasımağa formation in previous works (Bilgin et al., 1986) were determined to be the ultramafic-mafic rocks within the ophiolitic complex which were affected from the granitic rocks.

Lithologies of the Kasımağa formation (Bilgin et al., 1986) observed around the Kasımağa village were traced in that area (field no. IV) and based on their lateral and vertical transition with the ophiolitic complex out of the study area (Akyürek et al., 1984), they are believed to be laterally changing to the complex within the area.

Lithologies to be included to the Eocene Çayraz formation were determined in the area (field no. I). Moreover, it is determined in the present study that limestones of the Çayraz formation are technically exposed at the basement of the İncik formation and they are positioned as blocks within the İncik formation (field no. I).

Considering the lateral and vertical transition between Miocene-Pliocene (?) volcanic rocks (field no. IV) and İncik formation out of the study area (Akyürek et al., 1984), they are believed to be laterally transitional within the area.

Detail mapping of lithologies of the Kızılırmak formation that comprises most part of the study area, determining of their relation to the İncik formation, and necessity of differentiation of both formations from each

other are the purposes of present study. It is believed that at least, some part of widely exposing lithologies mapped as Kızılırmak formation may be included to the İncik formation.

## BASIN EVOLUTION MODEL

Considering the studies conducted so far, evolution of basin may be schematized as follows:

In the basin evolved during the upper Cretaceous,. sedimentary and volcanic- volcaniclastic rocks transitional with the ophiolitic melange were deposited over the basement consisting of lithologies unique to Kırşehir massive of Paleozoic-Mesozoic age. Basement rocks are intruded by Maastrichtian-Paleocene granitoids. They are unconformably covered with Eocene-Quaternary post-tectonic basin deposits.

## BRIEF INFORMATION ABOUT THE DEPOSIT

Kesikköprü iron deposit is located 35 km from the southern junction of the Ankara-Kaman highway at 100th km.

There are a total of 8 deposits and occurrences in the region. Of these, Madentepe I, Madentepe II, and Suluocak deposits are presently operated in field no. I while Büyükocak, Adilocak, Kartalkaya I, Kartalkaya II, and Camiisagir pits are already abandoned. Due to their exploitability and having similar features with other occurrences, well samples and samples collected from Madentepe I, Madentepe II, and Suluocak pits will be examined in detail.

The mineralization in the Kesikköprü iron deposit and occurrences is observed as lenses of different sizes (- 100 x 20 x 10 m) around or at the contacts between crystallized limestone, ultramafic-mafic rocks, and granitic rocks. Ore minerals are magnetite and lesser amount of hematite, limonite and trace amounts of pyrite. In general, Fe contents 45-65%, $SiO_2$ contents are 10-15%, and S contents are 1-2%. These ore lenses comprise masses ranging from 20 thousand to 5 million tones and have a reserve of about 11 million tones (Öztürk et al., 1983). Faults detected around the pits are in NW-SE direction and give rise to transportation of ore-bearing fluids.

## PETROGRAPHY OF DRILLING SAMPLES

A total of 481 core samples was systematically collected from a number of 10 wells drilled in the Kesikköprü iron deposit by MTA in the years between 1977 and 1982. A total of-150 thin sections was systematically prepared from the Kes-2 well in which ore-country rock relation is well displayed. As a result of macroscopic and microscopic examinations, it was determined that the dominant rock type of the drilling with a depth of 173 m is generally gabbroic type mafic rocks that are partly subjected to hydrothermal alteration. In addition, altered ultramafic rocks were also observed.

### Mafic rocks

Examination of drilling samples from surface to depth reveals that in hand specimens to the first 100 m, light and dark colored mineral alternations are repeated in a narrow space and dark gray, gray, and green colored, partly fine grained materials with a tight appearance are dominated.

Microscopic investigations indicate the presence of polysynthetic twinnings in subhedral medium, fine, and very fine grained plagioclases and xenomorphic medium to fine grained plagioclases. In places, intense argillization and lesser amounts of serialization are also observed.

Diopside-augite type of clinopyroxenes of medium to fine grained, getting coarser in places, are also present. Fine grains are in euhedral and prismatic shapes and as the grain size gets coarse, they appear as subhedral and anhedral forms. They seem to be transformed to amphiboles along fracture and margins.

Medium to fine grained, subhedral, anhedral, platy hastingsite type pleochroic primary amphiboles are observed in light green and brown colors and ac-

company the pyroxenes. Moreover, fibrous, radial, bar-like tremolite type secondary amphiboles formed as a result of amphibolitization of pyroxenes are widely detected.

Medium to fine grained, subhedral, anhedral, disseminated three type opaque occurrences as thin veinlets are observed along the cleavage traces associated with amphibolitization of pyroxenes.

In addition, medium to fine grained, subhedral to anhedral, zoned, locally radial, green colored pleochroic tourmalines and xenomorphic, stockwork type yellowish brown colored, optic, isotropic garnet group minerals, and lesser amounts of fine grained xenomorphic epidot group minerals are also observed.

A granular texture is detected among the plagioclase and pyroxenes that are the main components of the rock. However, these two components display a distinctive banded texture as alternations of plagioclase and pyroxene in both hand specimens and thin sections (Plate I, fig. 1). This appearance may indicate the presence of a complex copsisting of ultramafic and mafic lithologies.

Mafic rocks subjected to hydrothermal alteration

In hand specimens from 100 to 130th meters of core samples, a fractured structure in light gray to white colors with intense carbonatization and magnetic susceptibility is distinctive.

The main components of the rock are composed of two different associations unique to the same rock that is subjected to hydrothermal alteration also accompanying the ore.

Opaque minerals are generally medium to coarse grained, subhedral to anhedral, subjected to cataclysm and observed as fractured and fissured and being replaced by hematite along the edges. Lesser amounts of fine grained, anhedral opaque minerals associated with carbonates are also detected.

In some of altered mafic rocks accompanying the ore, carbonate-rich levels are observed derived from carbonatization of light colored minerals (plagioclase). While in some samples, dark colored minerals show amphibolitization, carbonatization, and lesser amount of chloritization signs. These transformations are detected even only one thin section.

Along the fracture and fissures of medium to fine grained, anhedral light brown opaque minerals, two types of carbonates are observed: one is iron-rich ankerite type carbonates and another is coarse, medium, and fine grained, anhedral calcite type carbonates, in those of coarse to medium grained, pressure twinnings are also observed. A little amount chlorite filled space is also detected in the rock.

In other samples showing amphibolitization, carbonatization, and little amount of chloritization, a large amount of pyroxene relicts together with tremolites formed a result of amphibolitization of pyroxenes are observed. Tremolites are fine to medium grained, platy, fibrous, locally radial, chloritized, and intensely carbonaceous.

Ultramafic rocks subjected to hydrothermal alteration

In hand specimens from 130 to 165th meters of core samples, they are observed as light gray to beige colored, schistose carbonaceous levels.

Completely carbonated serpentines with a distinctive sieve texture, which also locally bear relicts of opaque minerals, comprise the main component of the rock. In the places of intense serpentinization, a significant orientation is observed (Plate I,fig. 2).

Two different carbonate types were determined in the rock. First is fine, medium to coarse grained, subhedral to anhedral calcite type carbonates with widespread pressure twinnings, while the second is fine grained, anhedral, light brown colored ankerite type carbonates particularly accumulated where serpentinization is present.

Opaque minerals as fine to medium grained, euhedral, subhedral disseminations are detected together with veins associated with serpentinization (Plate I, fig. 3). In disseminated opaque minerals, silicate minerals are observed along cleavage traces and fractures (Plate I, fig. 4).

Samples from 165 to 173rd meters of well are composed of light green-beige colored, fine grained rocks of tight appearance and mostly resemble hydrothermally altered mafic rocks. These levels in previous studies are evaluated as "skarn occurrences" and/or fels (Öztürk et al., 1983). In these levels, medium to coarse grained, euhedral to subhedral, locally anisotropic lamellae-bearing, optically isotropic garnet type minerals and light green colored, fine to medium grained, subhedral, fibrous, pleochroic epidot group minerals together with lesser amounts of fine grained euhedral to subhedral, prismatic pyroxenes also observed. In addition, within the pores of the rock, green colored, pleochroic possibly iron-rich chlorites together with quartz are also detected.

## ORE MINERALOGY

As a result of petrographic examinations of the surficial and drilling samples collected around the Kesikköprü iron deposit, a total of 29 polished sections was prepared, from 9 source rock and 4 country rock samples, 4 samples from the pits, and 12 from ore samples, and described with the ore microscopy. Non-opaque minerals accompanying opaque minerals were also examined with thin sections prepared parallel to polished sections.

### Ultramafic and mafic rocks

Ore microscopy examinations of ultramafic rocks were performed under two different rock assemblages as peridotite and serpentinite type rocks and gabbro-diabase type rocks together with pyroxenite resembling the composition of ultramafic rocks. It was also determined that, like in the silicate minerals, ore minerals of ultramafic rocks display similarities. Therefore, textural and compositional relations in the ore minerals of both groups are presented on the basis of each ore mineral.

*Peridotite and serpentinites.* - These source rocks are represented with dunite, harzburgite, lherzolite, and sefpentinites of peridotite family.

Microscopic examinations reveal that coarse grained, euhedral to subhedral, chromites locally subjected to an intense cataclysm appear to be transformed to chrome spinel and magnetite along fracture, fissure, and edges (Plate I, fig. 5).

Magnetites of the rock can be divided into 4 groups. 1 st group is observed as transformation of chromites to magnetite along fracture, fissure, and edges, 2nd group is detected as fine grained, anhedral, skeleton- and veinlet-shaped, silicate inclusion-bearing magnetites within serpentines, 3rd group appears to be fine grained, subhedral to anhedral, magnetites along the cleavage plains of orthopyroxenes (Plate I, fig. 6), and 4th group is observed as fine grained, anhedral, cloudy magnetite grain accumulations appearing along the cleavage plains of orthopyroxenes as a result of serpentinization. Moreover, transforming of magnetite occurrences to maghemite and mushketovite are also frequently observed.

Magnetites together with lesser amounts of fine grained, anhedral, pyrite occurrences are detected along the cleavage plains of serpentinized orthopyroxenes.

Chalcopyrites surrounded by magnetites are generally observed as fine grained and subhedral to anhedral. They are intensely subjected to limonitization.

Fine grained, anhedral pyrrhotite is also found in the rock.

Lesser amounts of pentlandite-gersdorffite are generally associated with fine grained, subhedral to anhedral and rarely with euhedral magnetite. Mackinawite fibers are detected within pentlandites and along its cleavages (Plate II.fig. 1).

Siderite and ankerites are observed as veinlets locally being transformed to goethite and limonite. Little amount of goethite and limonite occurrences is also found as transformation of chalcopyrites to limonite.

*Pyroxenite-gabbro and diabases.-* Rocks of this group is characterized by pyroxenite, plagioclase pyroxenite, websterite, gabbro, spinel gabbro, olivine gabbro, and diabase. Although pyroxenites are associated with ultramafic rocks, they also exhibit transition to mafic rocks.

Subhedral, anhedral, skeleton-shaped magnetites are observed along the cleavage plains, fracture, and fissures of orthopyroxenes. They are transformed to hematite as a result of intense martitization. In some cases, magnetites seem to be associated with garnets (hydrogrossular ?: rodingitization ?) both formed in diopside and augite.

Chalcopyrites are generally fine grained, mostly subhedral, rarely anhedral, and intensely subjected to limonitization.

Fine grained, subhedral, anhedral spinel minerals (possibly hercynite) are rarely developed along the cleavage plains of orthopyroxenes (Plate Il, fig. 2).

In addition, lesser amount of pentlandite, chromite, ilmenite, and sphene together with secondary limonitization are also observed.

### Ore properties

Petrography and XRD studies reveal that gangue minerals of the ore samples are generally composed of chlorite, tremolite-actinolite, carbonate minerals, pyroxene, and lesser amounts of garnet, quartz, and clay minerals, and in some cases, talc and little amount of olivine which are vitally important in origin.

In order of abundance, ore minerals can be listed as follows:

Magnetites may be examined under 4 different groups. 1 st group is composed of fine grained silicate inclusion-bearing magnetites (Plate Il, fig. 3) and they gradually change to magnetites with no inclusion to the crystal margins and form zoning matrix. 2nd group is coarse grained, subhedral to anhedral, sutured, and has a cataclastic structure and has been widely changed to martite along fracture, fissure, and cleavage plains (Plate Il, fig. 4). 3rd group is composed of fine grained, anhedral, cloudy magnetites in which coarse grained magnetites appear to fill the spaces. They change to martite in places. 4th group is observed as fine to medium grained, euhedral to subhedral, skeleton- and lattice-shaped magnetites that are mostly replaced by siderite and ankerites.

A little amount of fine to medium grained, subhedral, chalcopyrite was determined to be associated with magnetite within siderite and ankerites. Tremolite, actinolite, and chlorite type silicate inclusions are found in magnetite and chalcopyrite and they seem to change to chalcocite, bornite, and covelline along their edges (Plate Il.fig. 5).

Fine graine, euhedral to subhedral, anhedral pyrites traversing the magnetites contain silicate inclusions.

Little amount of fine grained, subhedral, chromite in calcite and dolomite is completely changed to chrome spinel and magnetite along the edges (Plate Il, fig. 6).

Siderite-ankerite veins are observed in fracture and fissures of ore minerals also as replacing magnetites.

Lesser amounts of limonite formed as a result of surficial alteration is detected in magnetites.

## COMPARISON OF ORE MINERALOGY AND PETROGRAPHY STUDIES

Data obtained from ore mineralogy studies were compared with those from source and country rock petrography studies.

Considering rock systematic, there is a large consistency between petrography and ore mineralogy stu-

dies. Findings of ore mineralogy of source rocks and ore samples are also well in accordance with each other.

Primary mangetites in serpantinites are represented with fine grained, silicate inclusion-bearing magnetite occurrences. They are recrystallized as pure mangetites due to indirect effect of granitic rocks, that is by the effect of hydrothermal convection systems providing the fluid circulation within the country rocks heated by the granitic rocks, while fine grained silicates in magnetites give rise to crystal growths of coarse grained non-opaque minerals. During this process, depending on O and S fugacities, magnetites change to hematite also accompanied by pyrites. Thus, hydrothermally altered serpantinites are formed and hydrothermal alteration causes siderite, ankerite, and/or dolomite and calcite minerals to form as a result of reactions between mobile iron element and carbonatization which is another important characteristic of the system, like silicification. It is believed that most of the iron-carbonate minerals are formed by metasomatic effect of iron element leached from former magnetite and iron silicates.

During the hydrothermal alteration process, particularly mafic rocks and rocks with Ca-rich minerals give easily rise to formation of "skarn type" components. At the same time, cements of diabase type rocks may largely develop fels-like textures. However, it should also be considered that small relicts of limestones being observed as blocks within ultramafic and mafic rocks may also form country rock and lay the groundwork for skarn minerals.

As the loss on ignition of the whole rock increases (it is generally -2%, but it may be up to 4-5% or 7-9%, Table 1), impact of hydrothermal alteration is also increased. This, in turn, provides change of magnetites to hematite via martitization and/or bounding of iron element to the carbonates as vein type mineralizations traversing the structure. Late stage magnetite veinlets cut all the components. However, as the impact of hydrothermal alteration is decreased, that is rate of loss on Ignition is lowered, magnetites become stable to be observed in serpantinites.

Tourmaline-bearing veinlets that are believed to be associated directly with granitic fluids traverse the structures mentioned above. However, isolated states of such veinlets (separate from other gangue minerals) indicate that they have no direct effect on the mineralization. Traversing of these veinlets through the hydrothermal alteration matrix, that is fed by hydrothermal convection systems, may indicate that granitic rocks in the region have different ages but are derived from the same thermal conduit with different compositions.

## GEOCHEMISTRY

### Sampling and analysis method

Geochemical analyses were performed on a number of 25 selected samples collected from ore (12 samples), source and country rocks (13 samples) of the Kesikköprü iron deposit. The sampling localities are given in Doğan (1996).

Chemical analyses were carried out at the laboratories of the General Directorate of Mineral Research and Exploration of Turkey (MTA). Si, Ti, Al, Fe, Ca, K, and P elements were determined by XRF (X-ray Fluorescence method) while Mg, Na, Mn, Cr, Co, B, Sc, and Pb concentrations were found with AAS (Atomic Absorption Spectrophotometry) and OSA (Optical Spectral Analysis), loss on ignition and Cl with gravimetry, S element with Leco method (Iodimetric), N, Cu, Zn, Ba, Sr, Zr, V, La, Ga, Y, Nb, Ce, and Nd elements were determined by ICP (Induced Coupled Plasma) method. Detection limits of the instruments are given in Doğan (1996). As a result, chemical analyses of 11 major and 20 trace elements for 25 samples were obtained.

### Presentation of results of chemical Analysis

Results of chemical analysis of the samples collected from Kesikköprü iron deposit are shown in Table 1.

**Table 1- Chemical analyses results of source-country rock and ore samples of the Keskikköprü iron deposit ($Fe_2O_3$ total iron, G: conceration below the detection limit of the instrument).**

| | SOURCE ROCKS | | | | | | | | COUNTRY ROCKS | | | | | ORE | | | | | | | | | | |
|---|---|---|---|---|---|---|---|---|---|---|---|---|---|---|---|---|---|---|---|---|---|---|---|---|
| No | 1 | 2 | 3 | 4 | 5 | 6 | 7 | 8 | 9 | 10 | 11 | 12 | 13 | 14 | 15 | 16 | 17 | 18 | 19 | 20 | 21 | 22 | 23 | 24 | 25 |
| Sample Number | 93.S.10 | 93.S.11 | 93.S.14 | 93.S.16 | H-1 | H-5 | H-33 | H-34 | H-35 | Ç-18 | Ç-19 | K-11 | BE-9 | K-21 | K-25 | K-35 | Ç-30 | Ç-33 | Ç-40 | Ç-49 | SD-42 | 92.D.13 | 92.D.14 | 92.C.7 | 92.X.1 |
| Lithology | Dunite | Serpentin. | Harzburg.-Lherzolite | Websterite | Lherzolite | Spinel-Gabbro | Wehrlite-Lherzolite | Lherzolite | Websterite | Pyroxenit | Plagioc.-Pyroxenit | Gabbro | Diabase | Magnetit.-Pyrites | Magnetit. | Magnetit. | Magnetit. | Magnetit.-Pyrites | Magnetit.-Pyrites | Magnetit. | Magnetit. | Magnetit. | Magnetit. | Magnetit. | Magnetit. |
| Major Element (%) | | | | | | | | | | | | | | | | | | | | | | | | | |
| $SiO_2$ | 37,50 | 37,50 | 43,00 | 46,00 | 43,50 | 45,60 | 36,50 | 42,00 | 51,50 | 52,50 | 52,00 | 51,30 | 51,00 | 12,50 | 6,00 | 2,60 | 3,80 | 5,20 | 13,80 | 3,80 | 16,50 | 20,50 | 14,50 | 20,50 | 9,00 |
| $TiO_2$ | < 0.10 | < 0.10 | 0,10 | 0,10 | 0,10 | 0,10 | 0,10 | 0,10 | 0,10 | 0,10 | 0,10 | 0,20 | 0,50 | < 0.10 | < 0.10 | 0,10 | < 0.10 | < 0.10 | < 0.10 | 0.10 | < 0.10 | < 0.10 | < 0.10 | 0,10 | 0,10 |
| $Al_2O_3$ | < 0.10 | < 0.10 | 3,40 | 3,40 | 2,80 | 18,00 | 1,90 | 3,50 | 4,00 | 3,80 | 8,00 | 7,40 | 16,00 | < 0.10 | < 0.10 | 1,20 | < 0.10 | < 0.10 | < 0.10 | < 0.10 | < 0.10 | < 0.10 | 1,30 | 2,20 | < 0.10 |
| $Fe_2O_3$ | 16,10 | 14,10 | 14,00 | 11,50 | 14,00 | 6,80 | 17,50 | 14,00 | 8,40 | 5,20 | 4,50 | 3,80 | 5,80 | 78,26 | 86,26 | 86,53 | 94,60 | 81,60 | 72,12 | 81,30 | 64,66 | 59,84 | 69,46 | 51,39 | 77,32 |
| MnO | 0,37 | 0,25 | 0,32 | 0,28 | 0,27 | 0,17 | 0,25 | 0,26 | 0,22 | 0,31 | 0,22 | 0,21 | 0,34 | 0,09 | 0,09 | 0,45 | 0,25 | 0,23 | 0,22 | 0,34 | 0,27 | 0,15 | 0,37 | 0,15 | 0,27 |
| MgO | 31,00 | 34,00 | 25,00 | 24,00 | 26,00 | 11,50 | 28,00 | 28,00 | 18,00 | 13,80 | 11,50 | 12,00 | 5,50 | 3,10 | 2,60 | 3,20 | 1,40 | 3,30 | 5,50 | 2,30 | 4,80 | 8,50 | 1,60 | 12,50 | 1,90 |
| CaO | 2,30 | 1,70 | 9,40 | 12,00 | 7,10 | 15,60 | 3,80 | 6,80 | 15,50 | 21,00 | 21,50 | 20,50 | 16,00 | 5,70 | 4,50 | 3,00 | 1,80 | 3,20 | 1,90 | 3,80 | 7,50 | 11,00 | 10,00 | 3,80 | 8,20 |
| $Na_2O$ | 0,05 | < 0.01 | 0,18 | 0,16 | 0,05 | 0,38 | 0,01 | 0,09 | 0,25 | 0,60 | 0,40 | 0,30 | 3,00 | 0,01 | < 0.01 | 0,01 | < 0.01 | < 0.01 | 0,02 | 0,02 | 0,02 | < 0.01 | < 0.01 | < 0.01 | < 0.01 |
| $K_2O$ | 0,10 | < 0.10 | 0,10 | 0,10 | < 0.10 | 0,10 | < 0.10 | < 0.10 | 0,10 | 0,10 | 0,10 | 0,20 | 0,10 | < 0.10 | < 0.10 | 0,10 | < 0.10 | < 0.10 | < 0.10 | 0,10 | < 0.10 | < 0.10 | < 0.10 | < 0.10 | < 0.10 |
| $P_2O_5$ | < 0.10 | < 0.10 | < 0.10 | < 0.10 | < 0.10 | < 0.10 | < 0.10 | < 0.10 | < 0.10 | < 0.10 | 0,10 | 0,20 | 0,10 | < 0.10 | < 0.10 | < 0.10 | < 0.10 | < 0.10 | < 0.10 | < 0.10 | < 0.10 | < 0.10 | < 0.10 | < 0.10 | < 0.10 |
| Loss On Ignitions (LOI) | 9,04 | 11,48 | 4,50 | 2,84 | 7,00 | 1,72 | 9,52 | 7,10 | 1,95 | 2,25 | 1,15 | 1,50 | 1,40 | 1,85 | 1,85 | 1,55 | 1,20 | 4,00 | 7,05 | 8,10 | 4,40 | 2,00 | 2,80 | 6,95 | 3,75 |
| Total | 97,27 | 99,33 | 100,07 | 100,45 | 99,97 | 100,04 | 99,72 | 99,99 | 100,00 | 99,43 | 99,67 | 97,81 | 99,74 | 99,89 | 101,59 | 101,11 | 103,34 | 98,82 | 100,89 | 100,10 | 100,63 | 100,28 | 100,05 | 99,74 | 100,78 |
| Trace Element (ppm) | | | | | | | | | | | | | | | | | | | | | | | | | |
| Cr | 2300 | 2600 | 1000 | 900 | 700 | 400 | 700 | 700 | 1900 | 1100 | 1300 | 1400 | 600 | G | 70 | 70 | 70 | 180 | 70 | 40 | 200 | 70 | 100 | 100 | 70 |
| V | 71 | 50 | 120 | 151 | 100 | 115 | 55 | 86 | 200 | 139 | 54 | 177 | 211 | G | 72 | 59 | G | G | G | 116 | G | G | 57 | G | 91 |
| Ni | 724 | 1156 | 445 | 470 | 456 | 350 | 556 | 467 | 288 | 478 | 148 | 448 | 232 | 135 | 130 | 282 | 188 | 457 | 202 | 820 | 513 | 304 | 404 | 202 | 320 |
| Co | 700 | 900 | 900 | 70 | 70 | G | 70 | 70 | 70 | G | G | G | G | 70 | 70 | G | 70 | 150 | 150 | 40 | 40 | 40 | G | G | G |
| Cu | 59 | 14 | 661 | 47 | 39 | 101 | 43 | 44 | 33 | 25 | 44 | 147 | 94 | 114 | 16 | 51 | 18 | 1062 | 361 | 98 | 46 | 63 | 154 | 26 | 34 |
| Zn | 227 | 142 | 209 | 107 | 165 | 120 | 199 | 138 | 180 | 121 | 207 | 157 | 119 | 250 | 299 | 161 | 328 | 310 | 272 | 151 | 334 | 357 | 292 | 132 | 218 |
| S | 1400 | 200 | 800 | 200 | 200 | 200 | 100 | 200 | 100 | 100 | 2400 | 200 | 200 | 24000 | 100 | 100 | 300 | 24000 | 25500 | 300 | 100 | < 10.000 | 300 | 100 | 400 |
| Cl | < 500 | < 500 | < 500 | < 500 | < 500 | < 500 | < 500 | < 500 | < 500 | < 500 | < 500 | 700 | < 500 | < 500 | < 500 | < 500 | < 500 | < 500 | < 500 | < 500 | < 500 | < 500 | < 500 | < 500 | < 500 |
| Ba | 21 | 12 | 26 | 63 | 84 | 114 | 46 | 53 | 80 | 38 | 18 | 20 | 23 | 20 | 21 | 22 | 46 | 87 | 37 | 26 | 36 | 30 | 34 | 35 | 38 |
| Pb | 70 | G | G | 40 | G | 70 | G | G | G | 40 | 40 | G | 100 | G | G | G | G | G | G | 40 | 40 | G | G | G | G |
| Sr | 29 | 15 | 18 | 132 | 21 | 76 | 74 | 22 | 23 | 257 | 46 | 20 | 99 | 60 | 60 | 74 | 144 | 126 | 109 | 130 | 97 | 66 | 127 | 84 | 108 |
| Zr | G | G | G | 164 | G | G | G | G | G | 87 | G | G | G | G | G | G | G | G | G | G | G | G | G | G | G |
| B | 70 | 70 | 40 | G | 70 | G | 200 | 40 | 40 | 150 | 1500 | 2000 | 150 | G | G | G | G | G | G | G | G | 40 | G | G | G |
| Sc | G | G | 150 | 70 | 40 | 70 | G | G | 100 | 150 | 100 | 100 | 40 | G | G | G | G | G | G | G | G | G | G | G | G |
| La | G | G | G | G | G | G | G | G | G | 90 | G | G | G | G | G | G | G | G | G | G | G | G | G | G | G |
| Ga | G | G | G | G | G | G | G | G | G | G | G | G | G | G | G | G | G | G | G | G | G | G | G | G | G |
| Y | G | G | G | G | G | G | G | G | G | G | G | G | G | G | G | G | G | G | G | G | G | G | G | G | G |
| Nb | G | G | G | G | G | G | G | G | G | G | G | G | G | G | G | G | G | G | G | G | G | G | G | G | G |
| Ce | G | G | G | G | G | G | G | G | G | G | G | G | G | G | G | G | G | G | G | G | G | G | G | G | G |
| Nd | G | G | G | G | G | G | G | G | G | G | G | G | G | G | G | G | G | G | G | G | G | G | G | G | G |
| M.T.A. Analy. Lab. No. | 62495 | 62496 | 62497 | 62498 | 62499 | 62500 | 62501 | 62502 | 62503 | 62504 | 62505 | 62506 | 62507 | 62508 | 62509 | 62510 | 62511 | 62512 | 62513 | 62514 | 62515 | 62516 | 62517 | 62518 | 62519 |

Maximum, minimum, and mean values together with standard deviations for the samples are displayed in Table 2a and b.

Since quantitative evaluation of analyses results is quite difficult, they were examined with graphical and geostatistical methods which are given in the following

Table 2a- Maximum, minimum, standard deviation, and mean values of source and country rocks. The numbers given in parenthesis below the mean value stand for the number of samples. Minimum values for the elements not detected were statistically evaluated based on 70% of the detection limit of the instrument for the relevant element, n.d.: not determined.

| MAJOR OXIDES (%) | | | | | | | | | | |
|---|---|---|---|---|---|---|---|---|---|---|
| | $SiO_2$ | $TiO_2$ | $Al_2O_3$ | $Fe_2O_3$ | MnO | MgO | CaO | $Na_2O$ | $K_2O$ | $P_2O_5$ | LOI |
| Minimum Value | 37.50 | 0.07 | 0.10 | 3.80 | 0.17 | 5.50 | 1.70 | 0.01 | 0.07 | 0.07 | 1.15 |
| Maximum Value | 52.50 | 0.50 | 16.00 | 17.50 | 0.37 | 34.00 | 21.50 | 3.00 | 0.20 | 0.20 | 11.57 |
| Standard Deviation | 5.72 | 0.11 | 5.57 | 4.83 | 0.06 | 8.88 | 7.06 | 0.79 | 0.03 | 0.04 | 3.68 |
| Mean Value | 45.55 (13) | 0.13 (13) | 5.57 (13) | 10.44 (13) | 0.27 (13) | 20.38 (13) | 11.83 (13) | 0.42 (13) | 0.10 (13) | 0.08 (13) | 4.76 (13) |

| TRACE ELEMENTS (ppm) | | | | | | | | | | | |
|---|---|---|---|---|---|---|---|---|---|---|---|
| | Cr | V | Ni | Co | Cu | Zn | S | Cl | Ba | Pb | Sr |
| Minimum Value | 400 | 50 | 148 | 28 | 14 | 107 | 100 | 350 | 12 | 28 | 15 |
| Maximum Value | 2600 | 211 | 1156 | 700 | 881 | 307 | 2400 | 700 | 114 | 100 | 257 |
| Standard Deviation | 663 | 55 | 250 | 180 | 232 | 56 | 679 | 97 | 33 | 23 | 69 |
| Mean Value | 1208 (13) | 119 (13) | 478 (13) | 107 (13) | 116 (13) | 171 (13) | 469 (13) | 377 (13) | 47 (13) | 43 (13) | 64 (13) |

| TRACE ELEMENTS (ppm) (Cont.) | | | | | | | | | |
|---|---|---|---|---|---|---|---|---|---|
| | Zr | B | Sc | La | Ga | Y | Nb | Ce | Nd |
| Minimum Value | 28 | 28 | 28 | 28 | n.d. | n.d. | n.d. | n.d. | n.d. |
| Maximum Value | 184 | 3000 | 150 | 90 | n.d. | n.d. | n.d. | n.d. | n.d. |
| Standard Deviation | 45 | 872 | 45 | 17 | n.d. | n.d. | n.d. | n.d. | n.d. |
| Mean Value | 45 (13) | 414 (13) | 72 (13) | 33 (13) | n.d. (13) | n.d. (13) | n.d. (13) | n.d. (13) | n.d. (13) |

Table 2b- Maximum, minimum, standard deviation, and mean values of ore samples, n.d.: not determined.

| MAJOR OXIDES (%) | | | | | | | | | | |
|---|---|---|---|---|---|---|---|---|---|---|
| | $SiO_2$ | $TiO_2$ | $Al_2O_3$ | $Fe_2O_3$ | MnO | MgO | CaO | $Na_2O$ | $K_2O$ | $P_2O_5$ | LOI |
| Minimum Value | 2.80 | 0.07 | 0.10 | 51.39 | 0.09 | 1.40 | 1.80 | 0.01 | 0.07 | 0.07 | 1.16 |
| Maximum Value | 20.50 | 0.10 | 2.20 | 94.60 | 0.45 | 12.50 | 11.00 | 0.02 | 0.10 | 0.07 | 8.97 |
| Standard Deviation | 6.61 | 0.01 | 0.70 | 12.48 | 0.11 | 3.09 | 3.11 | 4.52 | 0.01 | 0.00 | 2.69 |
| Mean Value | 11.00 (12) | 0.08 (12) | 0.47 (12) | 75.30 (12) | 0.24 (12) | 4.07 (12) | 5.37 (12) | 0.01 (12) | 0.08 (12) | 0.07 (12) | 3.94 (12) |

| TRACE ELEMENTS (ppm) | | | | | | | | | | | |
|---|---|---|---|---|---|---|---|---|---|---|---|
| | Cr | V | Ni | Co | Cu | Zn | S | Cl | Ba | Pb | Sr |
| Minimum Value | 28 | 28 | 130 | 28 | 16 | 132 | 70 | 350 | 20 | 28 | 60 |
| Maximum Value | 200 | 116 | 820 | 150 | 1082 | 357 | 25500 | 350 | 46 | 40 | 144 |
| Standard Deviation | 47 | 30 | 198 | 44 | 296 | 77 | 10998 | 0 | 8 | 5 | 30 |
| Mean Value | 87 (12) | 49 (12) | 330 (12) | 62 (12) | 169 (12) | 259 (12) | 6273 (12) | 350 (12) | 32 (12) | 30 (12) | 99 (12) |

| TRACE ELEMENTS (ppm) (Cont.) | | | | | | | | | |
|---|---|---|---|---|---|---|---|---|---|
| | Zr | B | Sc | La | Ga | Y | Nb | Ce | Nd |
| Minimum Value | 28 | 28 | n.d. | n.d. | n.d. | n.d. | n.d. | n.d. | n.d. |
| Maximum Value | 28 | 40 | n.d. | n.d. | n.d. | n.d. | n.d. | n.d. | n.d. |
| Standard Deviation | 0 | 4 | n.d. | n.d. | n.d. | n.d. | n.d. | n.d. | n.d. |
| Mean Value | 28 (12) | 29 (12) | G (12) | G (12) | G (12) | G (12) | G (12) | G (12) | G (12) |

sections. However, some points are needed to be explained for understanding of the evaluations.

Geochemical analyses performed on the samples from source and country rocks were compared with the; mean values of similar rock assemblages given in Table 3. Based on this, $SiO_2$ contents (37.50%) of dunite and serpantinite samples with sample nos. 1 and 2 are lower in comparison to those of normal harzburgite and dunite (Table 3) while their MgO contents are high while their MgO content is somewhat low. 3000-ppm B content of gabbro with sample no. 12 is also high. It is noticeable that pyroxenite with sample no. 11 and gabbro with sample no. 12 with the highest B contents (1500 and 3000 ppm, respectively) have the lowest total iron oxide contents of all, 4.50 and 3.80%, respectively. Cr, V, Ni, and Co contents of all source and country rock samples (sample nos. 1-13) are within the limit values of ultramafic and mafic rocks presented in Table 3.

Table 3- Some major and trace element contents of ultramafic and mafic rocks (Oman, Burro Mountain, Twin Sisters, and Troodos) (from Boudier and Coleman, 1981).

| | Harzburgite | Dunite | Websterite | Gabbro |
|---|---|---|---|---|
| Major Element (%) | | | | |
| $SiO_2$ | 43.50-44.00 (23) | 40.40-40.60 (16) | 48.30-54.30 (6) | 45.50-50.00 (8) |
| MgO | 45.30-46.20 (23) | 48.60-50.60 (16) | 13.00-17.60 (6) | 8.80-19.00 (8) |
| CaO | 0.50-0.91 (23) | 0.15-0.59 (16) | 12.60-20.50 (6) | 7.10-16.40 (8) |
| $Fe_2O_3$ | 7.20-8.20 (23) | 7.70-8.80 (16) | 3.00-4.30 (6) | 2.80-5.60 (8) |
| $Al_2O_3$ | 0.47-0.94 (23) | 0.14-0.63 (16) | 1.70-4.60 (6) | 5.70-18.30 (8) |
| $TiO_2$ | Not reported | Not reported | 0.05-0.14 (6) | 0.03-0.17 (8) |
| Trace Element (ppm) | | | | |
| Cr | 2669-3491 (23) | 2606-4107 (16) | 1780-8214 (6) | 411-4449 (8) |
| V | 20-60 (17) | 15-100 (14) | 115-194 (6) | 46-125 (8) |
| Ni | 2123-2830 (23) | 1887-3361 (16) | 670-1400 (6) | 515-1850 (8) |
| Co | 88-120 (17) | 96-140 (14) | 38-75 (6) | 38-80 (8) |

extremely low (31.00-34.00%). However, CaO values are somewhat high. Total iron oxide concentrations with 14.10-16.10% indicate an enrichment. CaO contents of lherzolites (sample nos. 3, 5, 7, and 8) show excess values while $Al_2O_3$ concentrations display a little increase. $SiO_2$, MgO, and total iron oxide relations of dunite and serpantinite samples are also valid for these samples. MgO contents of websterite (sample nos. 4 and 9) and pyroxenites (sample nos. 10 and 11) are a little higher while their total iron oxide concentrations are significantly higher when compared to those of websterite in Table 3. In addition, Sr contents of websterite with sample no. 4 (132 ppm) and pyroxenife with sample no. 10 (257 ppm) and B content of pyroxenite with sample no. 11 (1500 ppm) are significant. CaO and total iron oxide contents of spinel gabbro with sample no. 6 and gabbro with sample no. 12 are also

Except total iron content, $SiO_2$ (37.50-52.50%), MgO (5.50-34.00%), CaO (1.70-21.50%), $Al_2O_3$ (0.10-18.00), $Fe_2O_3$ (3.80-17.50%) contents of source and country rocks display a wide element distribution within the limits of ultramafic and mafic rocks. Low contents of $K_2O$, $P_2O_5$, $TiO_2$, MnO, and $Na_2O$ also accompany this association. Cr, V, Ni, Co, Cu, Zn, S, Cl, Ba, Pb, Sr, Zr, B, and Sc contents of source and country rocks are also variable. However, La, Ga, Y, Nb, Ce, and Nd contents of source and country rocks were not detected.

Total iron contents of ore samples in Table 2a are between 51.39 and 94.60% which are significantly higher than those of other elements. Their $Al_2O_3$ contents range from 0.10 to 2.20% and CaO contents are 1.80 and 11.00%, MgO contents are 1.40-12.50%, and $SiO_2$

contents are 2.80-20.50%. However, $Na_2O$, $K_2O$, and $P_2O_5$ contents are quite low. Cr, Ni, and Co contents are significant. Cu and Zn concentrations are somewhat high while Pb and Ba contents are significantly low. Another important point is that low B contents detected in ore samples (in whole rock analyses) are not consistent with Sc, La, Ga, Y, Nb, Ce, and Nd element contents.

## Interpretation of results of chemical analysis

A total of 13 major element geochemical data obtained from source and country rocks were plotted on the AFM diagram and compared with those on typical localities of ultramafic and mafic rocks. What is shown in this diagram that samples are generally concentrated along the FM axis and display some similarities to the ophiolitic rocks of Hatay region in Turkey (Doğan, 1996).

Careful examination of Table 1 reveals that MgO and $SiO_2$ contents of source and country rocks (sample nos. 1-13) are lower while their CaO contents are higher than those of ultramafic and mafic rocks at other localities. However, there is a significant increase (!) in their total iron oxide concentrations. Total iron oxide concentration of only a few samples display a decrease. Trace element content of source and country rocks are generally similar to those of ultramafic and mafic rocks at other localities. Table 1 displays the element behavior unique to serpentinite and hydrothermally altered serpentinite lithologies.

Ore samples (sample nos. 14-25) given in Table 1 resemble an iron ore with a wide range of major element concentration accompanied by Ca- and Mg-silicates. On the basis of whole rock analyses, particularly Zr, B, Sc, La, Ga, Y, Nb, Ce, and Nd trace element contents, that were not detected in ore samples, indicate that granitic fluids were not circulated in the ore or granitic rocks have no direct effect on the ore formation. However, high B but low total iron contents determined in only two country rock samples traversed by tourmaline veins may yield that granitic rocks possibly affected the system and they may be activated during at least one stage of frequently renewable iron element mobilization thus indicating that granitic rocks should not be precluded from the system. Absence of elements characterizing the granitic fluids within the ore rejects an iron expelling from granitic rocks or the model on iron enrichment deriving from granitic rocks.

Cr, V, Ni, and Co element enrichments in the ore samples indicate a possible genetic relation between mineralization and ultramafic-mafic rocks. Cu, Zn, S, and Ba contents may be due to hydrothermal circulation. Among the trace-elements, Cr has the most important role in the ore formation. Cr with a concentration range of 40-200 ppm in the ore samples seem to be a major element rather than a trace element and indicates the necessity of ultramafic-mafic rocks for the ore formation. Therefore, all samples (sample nos. 1-25) were reanalyzed at the laboratories of Ankara Nuclear Research and Training Center (ANRTC) (Sarayköy, Ankara) for their Cr contents. Table 4 shows Cr concentrations analyzed at the laboratories of both MTA and ANRTC. Cr contents of ore samples range from 36 to 113 ppm that absolutely indicate the necessity of ultramafic-mafic rocks for the ore formation.

**Table 4- Cr contents of source-country rock and ore samples analyzed with AAS method.**

| No. | Sample number | MTA (ppm) | ANRTC (ppm) |
|---|---|---|---|
| 1 | 93.S.10 | 2300 | 3362 ± 51 |
| 2 | 93.S.11 | 2600 | 3838 ± 103 |
| 3 | 93.S.14 | 1000 | 527.5 ± 36 |
| 4 | 93.S.18 | 900 | 495.5 ± 16 |
| 5 | H-1 | 700 | 376.5 ± 5 |
| 6 | H-5 | 400 | 246.5 ± 0.7 |
| 7 | H-33 | 700 | 327 ± 18.4 |
| 8 | H-34 | 700 | not analyzed |
| 9 | H-36 | 1800 | 1148 ± 29.7 |
| 10 | Ç-18 | 1100 | 222.5 ± 7.8 |
| 11 | Ç-19 | 1300 | 306.5 ± 0.7 |
| 12 | K-1 1 | 1400 | 429.5 ± 20.5 |
| 13 | BE-9 | 600 | 381.5 ± 3.5 |
| 14 | K-21 | n.d. | 36 ± 1.4 |
| 15 | K-26 | 70 | 39 ± 0 |
| 16 | K-35 | 70 | 59 ± 0 |
| 17 | Ç-30 | 70 | 47 ± 0 |
| 18 | Ç-33 | 150 | 1 13 ± 1.4 |
| 19 | Ç-40 | 70 | 49 ± 0 |
| 20 | Ç-49 | 40 | 39 ± 0 |
| 21 | SD-42 | 200 | 98 ± 0 |
| 22 | 92. D.13 | 70 | 58 ± 0 |
| 23 | 92.D.14 | 100 | 92 ± 1.4 |
| 24 | 92. C.7 | 100 | 53. 5 ± 0.7 |
| 25 | 92.X.1 | 70 | 63.5 ± 9.7 |

All the geochemical data yield that iron occurrences of hydrothermal origin are derived from ultramafic-mafic rocks and that serpentinization process has also contributed to the ore formation. The effect of granitic rocks on the system should not be neglected.

## Graphical presentation of results of analysis

Chemical analyses of 19 elements from 13 source and country rocks, 17 elements from 12 ore samples, and 22 elements from 25 whole rock samples were plotted on variation diagrams and distribution and trends between element pairs were determined. Thus, for each element pair consisting totally of 22 elements, a number of 538 variation diagrams were constructed with the use of computer.

Examination of variation diagrams of the element pairs of the Kesikköprü iron deposit reveals that there are similarities in distribution and trends of some element pairs. Since it is impossible to present all these graphics, considering their distribution relations and consistencies, only 7 positively correlated and 6 negatively correlated variation diagrams will be displayed (Figs. 3, 4, and 5). Correlation coefficients on the variation diagrams are separately presented in order to make distribution and trends more understandable.

It is shown in CaO vs. $SiO_2$ diagram of Fig. 3a that 13 source and country rock samples have similar trends. Graphic yields a positively correlated distribution extending from ultramafic to mafic rocks. V vs. $SiO_2$ diagram (Fig. 3b) shows that, except pyroxenite with sample no. 11, all the data points exhibit a positive correlation with a wide distribution from beginning. $SiO_2$ increase of sample nos. 10, 11, 12, and 13 is significant. It is shown in MgO vs. $Fe_2O_3$ diagram of Fig. 3c that 13 source and country rock samples display similar trends. Low Fe and Mg contents of sample nos. 10, 11,12, and 13 are significant. MgO vs. Ni diagram (Fig. 3d) shows a positively correlated distribution with a wide distribution from beginning. However, in the diagram, two different trends are observed. Diabase with sample no. 13, gabbro with sample nos. 6 and 12, pyroxenite with sample no. 10, and serpentinife with sample no. 2 display a trend parallel to that of pther samples. Mg and Ni contents of these samples are also low.

It is shown in $Fe_2O_3$ vs. CaO diagram of Fig. 3e that 13 source and country rock samples have similar trends. There is a negative correlation with a tight distribution from beginning. As CaO contents decrease from mafic to ultramafic rocks, $Fe_2O_3$ contents are increased. $SiO_2$ vs. $Fe_2O_3$ diagram of Fig. 3f indicates the presence of a negatively correlated distribution with a tight distribution from beginning. It is shown in $SiO_2$ vs. Ni variation diagram (Fig. 3g) that there is a negatively correlated distribution with a wide distribution from beginning. These diagrams also exhibit that $Fe_2O_3$ and Ni contents are decreased from ultramafic to mafic rocks. $Al_2O_3$ vs. MgO variation diagram (Fig. 3h) yields that, except gabbro with sample no. 6, all other samples have a negatively correlated distribution.

It is shown in $SiO_2$ vs. MgO variation diagram of Fig. 4a that 12 ore samples have similar trends. There is a positive correlated distribution with a wide distribution from beginning.

In the $Fe_2O_3$ vs. $SiO_2$ variation diagram of Fig. 4b, 12 ore samples show similar trends. In the diagram, there is a negative correlated distribution with a wide distribution from beginning.

There are two different parallel orientations in $SiO_2$ vs. CaO variation diagram of Fig. 5a constructed for 25 samples from source and country rocks. Ore samples at the left side of diagram yield a positive correlation with a wide distribution from beginning while source and country rock samples at the right side of diagram show a positive correlation with a tight distribution from beginning. In the MgO vs. Cr variation diagram of Fig. 5b, samples of ore, source and country rock samples indicate a positively correlated distribution with a wide distribution from beginning. Data points in these graphics may be evaluated as two separate parallel trends belonging to source and country rock samples.

There are two different trends in the variation diagram of $Fe_2O_3$ vs. $SiO_2$ built for ore, source, and country rock samples. However, these different variations se-

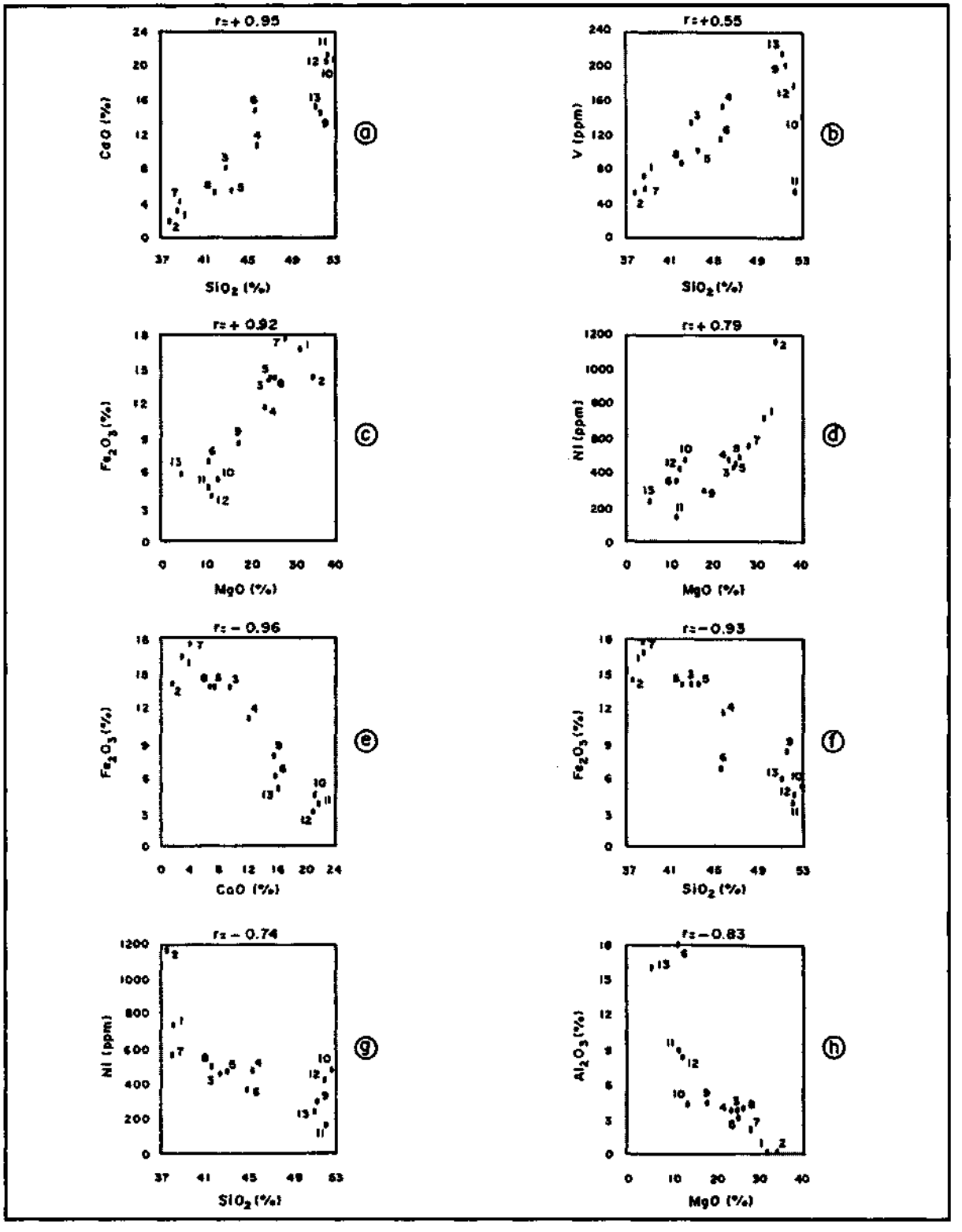


Fig. 3- Variation diagrams for different components of source and country rock samples.

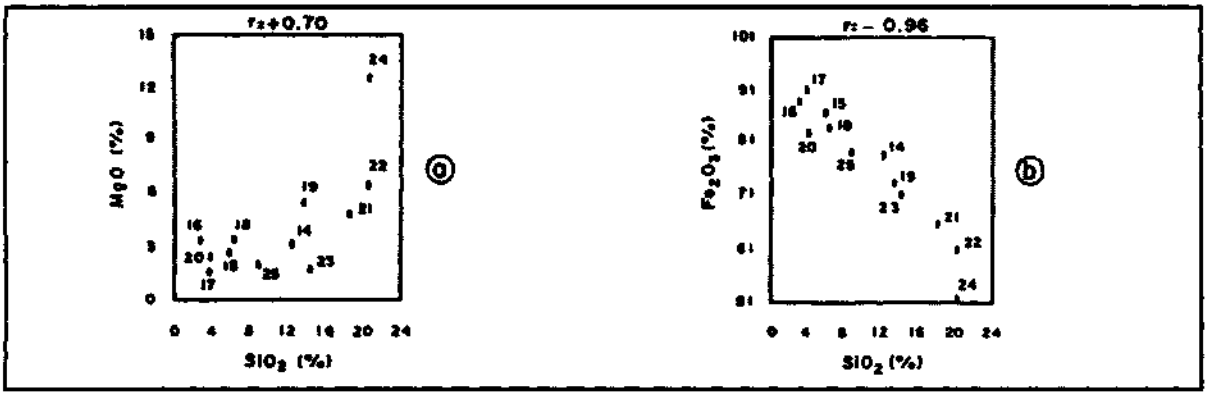


Fig. 4- Variation diagrams for different components of ore samples.

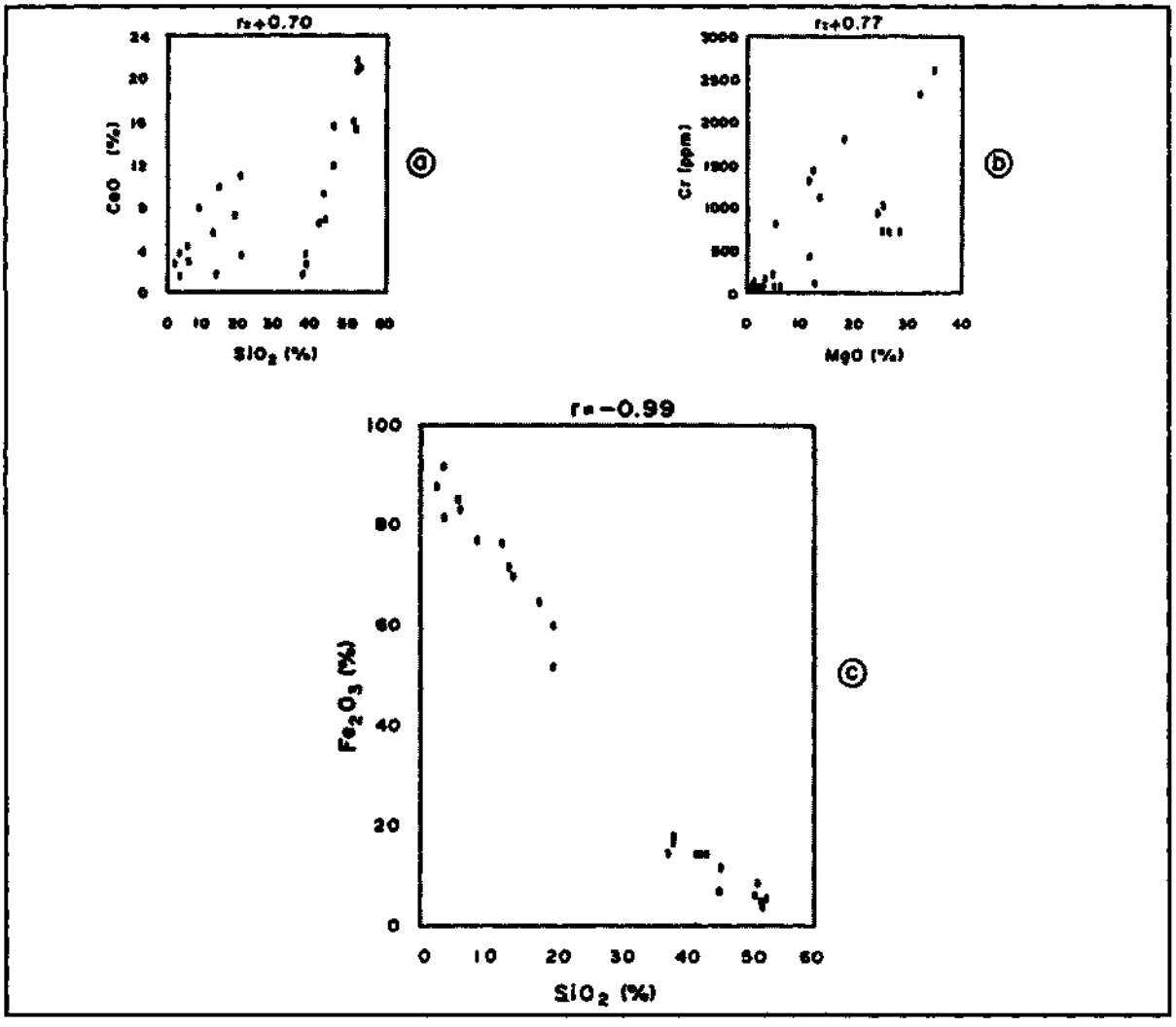


Fig. 5- Variation diagrams for different components of all samples (source-country rock and ore samples).

em to be continuation of each other. Samples yield a negatively correlated distribution (distribution of points observed along the same line) with a tight distribution from beginning.

### Interpretation of graphical presentations

In Fig. 6, a number of 10 graphics are presented that are selected out of 538 constructed based on source, country, ore, and whole rock samples.

At the top of Fig. 6, Ca-Si and Mg-Fe element groups are shown on first, second, and third rows of source and country rock graphics. These two groups inversely behave, in other words, they resemble the complex of ultramafic and mafic lithologies. In addition, Mg-Fe association indicates that iron element is dependent on ferromagnesian minerals in the source rocks.

At the center of graphics in Fig.6 constructed for ore samples, Mg-silicate forms a group. Contrary to the graphics of total iron oxide vs. MgO and the features observed in source rocks, there is a negatively correlated distribution. That is, iron element is differentiated from ferromagnesian minerals within the source rocks and becomes a source for iron minerals accompanied by Mg-silicates.

In the last row of Fig. 6, the variation diagram of $SiO_2$ vs. total iron oxide for all the samples are illustrated. Because, ultramafic and mafic rocks at one side and ore samples at another show almost the same trends with r = -1.00, in the diagram, the negative correlation with r = -0.99 is noticeable. Under these circumstances, searching of a source (e.g. granitic rocks) for the origin of iron element is unreasonable. The fact that laboratory methods are costly hinders the analyzing of granitic rocks. However, a distribution with r = -0.99 does not necessitate the performance of chemical analyses of granitic rocks.

### Geostatistics

Although a limited number of samples is available for the geostatistical methods to be applied, Cluster and Factor Analyses on the basis of linear regression were tested on different element pairs from a total of 25 samples (13 from source and country rocks and 12 from ore samples). Correlation coefficients of element pairs of 171 from source and country rocks, 136 from ore samples, and 231 from total samples were utilized. Considering high and medium and intermediate, positive, and negative correlation coefficients (Doğan, 1996), qualitative results and/or element group and associations are presented in Table 5.

In Table 5 in which Cluster Analyses were tested for source and country rocks, there seems to be two groups with a high positive correlation ($r > +0.65$). First group is represented with Ca, Si, and V elements. In this limited association, each three element behaves in the same way, that is if one of them increases, another also increases or vice versa. Second group of Table 5 with a,high positive correlation is characterized by Fe, Mg, Ni elements and loss on ignitions (LOI). Elements of second group behave with a positive correlation. They are also two groups with a positive correlation ($+0.65 > r > +0.40$) in the table. First group is composed of Ca, Si, V, Na, and Al elements. The difference of this association from the former first group that it includes Na and Al elements. Second group consists of Fe, Mg, Ni, Cr, Co elements and LOI. The main difference between the two second groups is that the latter group includes Cr and Co elements.

Two main groups with a high negative correlation ($r < -0.75$) appear in testing of Factor analyses for source and country rocks (Table. 5). First group is characterized by Ca, Si, and Al elements while second group is represented with Fe and Mg elements together with LOI. It seems that elements of first and second groups as a whole behave with a high positive correlation with respect to each other while elements of these groups display an association of a high negative correlation individually. In other words, as the elements of first group increase, elements of second group are decreased or vice versa. In last part of Table 5 belonging to source and country rocks, an association with an intermediate negative correlation ($-0.45 > r > -0.75$) is observed. Differing from the former first group with a high negative correlation, V and Na elements are included to the first group while Ni, Cr, Co, and Mn elements are included to the second group.

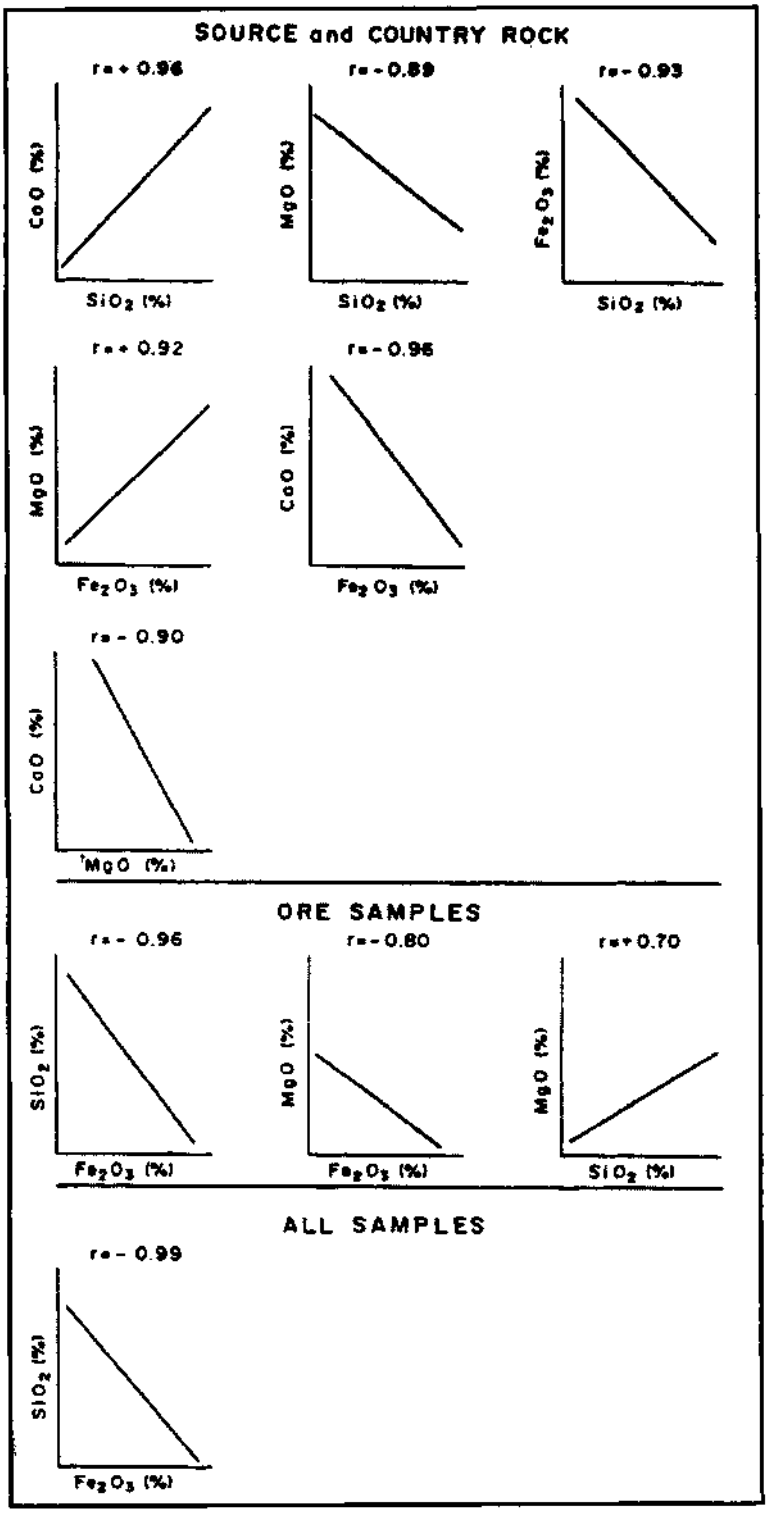


Fig. 6- Variation diagrams of some elements in source-country rock, ore, and whole rock samples. Distribution relations are characterized by regression lines and correlation coefficients.

**Table 5- Element group and associations and their possible origins.**

| | | |
|---|---|---|
| **SOURCE and COUNTRY ROCKS (for 13 samples)** | | |
| | r > +0.65 | |
| 1st Group: Ca, Si, V | | Mafic rocks |
| 2nd Group: Fe, Mg, Ni, LOI | | Ultramafic rocks |
| | +0.65 > r > +0.40 | |
| 1st Group: Ca, Si, V, Na, Al | | Mafic rocks |
| 2nd Group: Fe, Mg, Ni, LOI, Cr, Co | | Ultramafic rocks |
| | r < -0.75 | |
| Ca, Si, Al \|\| Fe, Mg, LOI | | |
| | | Complex of mafic and ultramafic |
| | -0.45 > r > -0.75 | lithologies |
| Ca, Si, Al, V, Na \|\| Fe, Mg, LOI, Ni, Cr, Co, Mn | | |

| | | |
|---|---|---|
| **ORE (for 12 samples)** | | |
| | r > +0.70 | |
| 1st Group: Mg, Si | | Silicate occurrences |
| | +0.70 > r > +0.30 | |
| 1st Group: Mg, Si, Ca, LOI | | Silicate (± corbonate) occurrences |
| 2nd Group: Ni, Mn | | Late hydrothermal effects |
| | r < -0.60 | |
| Mg, Si \|\| Fe | | |
| | | Silicate (± carbonate) |
| | -0.30 > r > -0.60 | occurrences and ore |
| Mg, Si, Ca, LOI \|\| Fe, Mn, Co, Zn | | |

| | | |
|---|---|---|
| **ALL SAMPLES (for 25 samples)** | | |
| | r > +0.73 | |
| 1st Group: Mg, Cr | | Ultramafic rocks |
| | +0.73 > r > +0.39 | |
| 1st Group: Ca, Si, V, Na, Al | | Mafic rocks |
| 2nd Group: Mg, Ni, LOI | | Ultramafic rocks |
| | r < -0.77 | |
| Si \|\| Fe | | Differentiation of iron associated |
| | -0.36 > r > -0.77 | with serpantinization |
| Mg, Cr, Ca, V \|\| Fe, Zn, LOI | | (Serpentinites subjected to Hydrothermal alteration) |

There is only one group with a high positive correlation ($r < +0.70$) appearing in testing of Factor analyses for ore samples (Table 5). This group is represented with Mg and Si elements. There are two groups in the table with an intermediate positive correlation ($+0.70 > r > +0.30$). First group is characterized by Mg, Si, Ca elements and LOI. The difference of this group from the former first group is the including of Ca ele-

ment and LOI. Second group is composed only of Ni and Mn elements.

Two main groups with a high negative correlation ($r < -0.60$) appear in testing of Factor analyses for ore samples (Table 5). First group consists of Mg and Si elements while second group is represented with only Fe element. In last part of Table 5 belonging to ore samples, an association with an intermediate negative correlation ($-0.30 > r > -0.60$) is observed. Differing from the former first group with a high negative correlation, Ca element and LOI are included to the first group while Mn, Co, and Zn elements are included to the second group.

There is only one group with a high positive correlation ($r < +0.73$) appearing in testing of Factor analyses for all samples (Table 5). This group is represented with Mg and Cr elements. There are two groups in the table with an intermediate positive correlation ($+0.73 > r > +0.39$). First group is characterized by Ca, Si, V, Na, and Al elements while second group is composed only of Mg and Ni elements together with LOI.

Two main groups with a high negative correlation ($r < -0.77$) appear in testing of Factor analyses for ore samples with (Table 5). First group is represented with only Si element while second group is represented with only Fe. In last part of Table 5 belonging to ore samples, an association with an intermediate negative correlation ($-0.36 > r > -0.77$) is observed. First group is represented with Mg, Cr, Ca, and V elements. Second group is composed of Fe and Zn elements together with LOI. Differing from the former second group with a high negative correlation, Zn element and LOI are included to the latter second group.

### XRD studies on core samples

Minerals found with XRD studies performed on 74 samples taken from Kes-2 well with a thickness of 173 m and the general petrographic features determined by microscope are described in Doğan (1996). In XRD studies, intensity values of each peak was also individually evaluated by the computer. Using the intensity values of 100 peaks, mineral components of each sample were semi-quantitatively calculated.

Quantitative distribution of main components of 74 samples from Kes-2 well determined with XRD studies is displayed in Fig. 7. Examination of the graphic reveals the presence of an association consisting of plagioclase, pyroxene, and hastingsite (plus tremolite) at the first 100-m part of the well. In the part to the depths from 100 meter, clay, quartz, calcite, dolomite, ankerite, siderite, and magnetite become dominant.

Correlation coefficients calculated on the basis of component pairs of 74 samples generally yield 3 different groups (Doğan, 1996). 1st group consists of magnetite, hematite, ankerite, and pyroxene minerals and comprises the ore-based group, 2nd group consists of tremolite, hastingsite, serpentine, and calcite minerals and comprises serpantinized lithologies and locally hydrothermally altered serpantinites, and finally 3rd group consists of only plagioclase and comprises plagioclase-rich lithologies. Minerals of each group display positive correlations while 2nd group minerals negatively correlate with those of 1 st and 3rd group minerals negatively correlate with those of 1st and 2nd group. This generalization indicates the presence of an alternation of plagioclase-rich lithologies at one side and the lithologies composed of altered mafic minerals (plus ore) at another side. In addition, correlation coefficients of some component variations were also computed such as hastingsite + tremolite = amphibole and hastingsite + tremolite + pyroxene = amphibole + pyroxene. This process yields the presence of 3 groups. 1 st group consists of hematite, magnetite, ankerite, siderite, and pyrite minerals and comprises the ore-based group, 2nd group consists of calcite, serpentine, and hastingsite + tremolite + pyroxene minerals and comprises serpantinized lithologies and locally hydrothermally altered serpantinites, and finally 3rd group consists of only plagioclase and comprises plagioclase-rich lithologies. Relations among these groups are similar to those of previously described ones. However, some increases in correlation coefficients are noticeable.

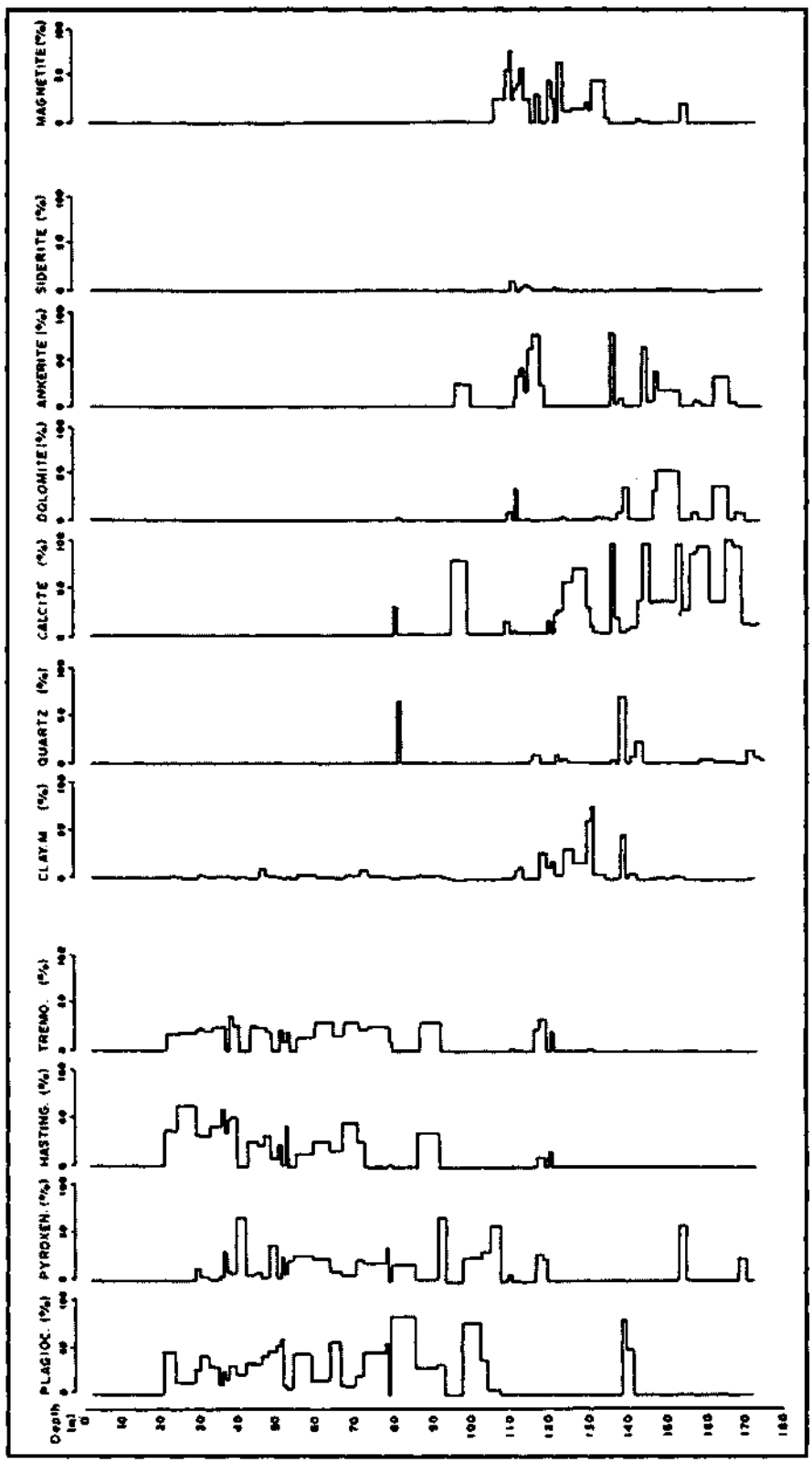


Fig. 7- Quantitative vertical distribution graphic of components from Kes-2 well samples.

Correlation coefficients of some major components and component variations are given in Table 6 that are based on 28 samples selected out of 74 core samples from plagioclase- and pyroxene-rich parts of the well to the depth of 100 m. The purpose is to clarify the relations among silicate components. Table 6 yields that hastingsite and tremolite display a positive correlation with respect to each other while pyroxene shows a negative correlation to both hastingsite and tremolite, and finally plagioclase has a negative correlation to all three minerals. In Table 6b, pyroxene shows a negative correlation with hastingsite + tremolite while plagioclase shows a negative correlation with hastingsite + tremolite and pyroxene. In Table 6c, there is a negative correlation between plagioclase and hastingsite + tremolite + pyroxene with r = -0.97. These circumstances reveal two original results. One is the change of hastingsites to tremolite. The second is sequential association among plagioclase, pyroxene, and hastingsites. Among the component percents in Fig 8, graphical presentation of distribution of plagioclase vs. hastingsite + tremolite + pyroxene is symbolically given.

Correlation coefficients of some major components and component variations are computed that are based on 27 ore samples selected out of 74 core samp-

Table 6- Correlation coefficients of component pairs for plagioclase- and pyroxenerich parts of well samples [a: plagioclase, tremolite, hastingsite, and pyroxene, b: plagioclase, hastingsite + tremolite (Amp) and pyroxene, c: plagioclase and hastingsite + tremolite + pyroxene (Amp-pyx) component variations].

| | Plg | Tre | Hst | Pyx |
|---|---|---|---|---|
| Plg | 1.00 | | | |
| Tre | -0.53 | 1.00 | | |
| Hst | -0.69 | 0.59 | 1.00 | |
| Pyx | -0.02 | -0.57 | -0.56 | 1.00 |

a

| | Plg | Amp | Pyx |
|---|---|---|---|
| Plg | 1.00 | | |
| Amp | -0.70 | 1.00 | |
| Pyx | -0.02 | -0.63 | 1.00 |

b

| | Plg | Amp-Pr |
|---|---|---|
| Plg | 1.00 | |
| Amp-Pr | -0.97 | 1.00 |

c

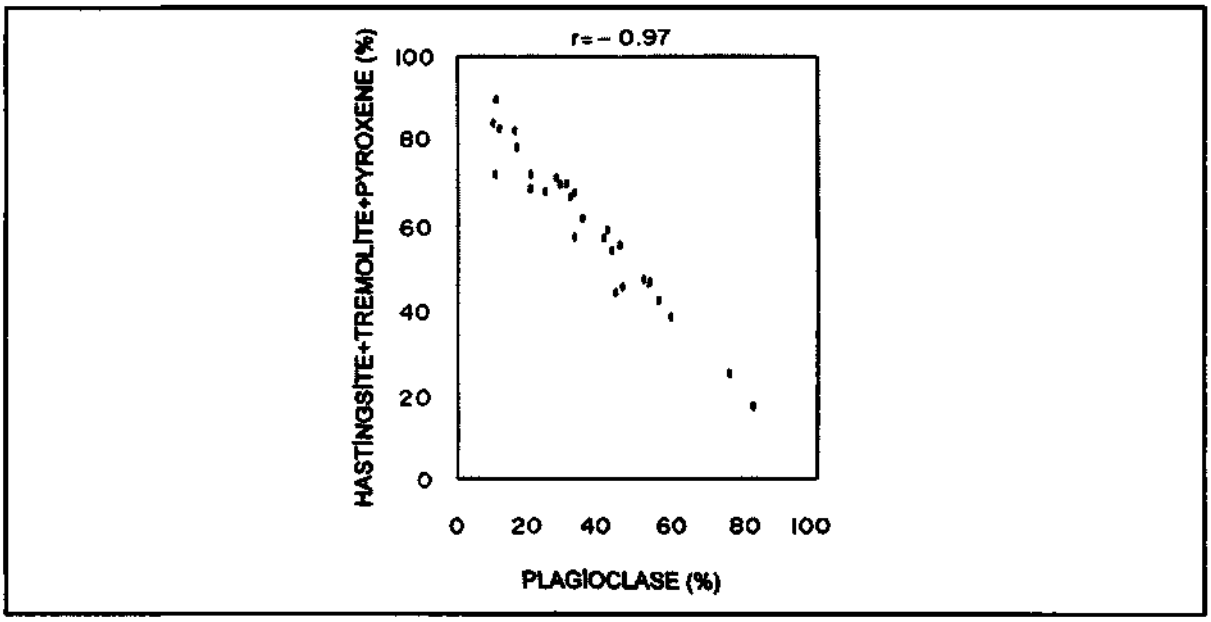


Fig. 8- Graphical presentation of plagioclase vs. hastingsite + tremolite + pyroxene distribution given in Table 60.

les from ore- and carbonate-rich parts of the well to the level deeper than 100 m (104.00-133.00 m). The purpose here is to clarify the relations among oxide-rich and carbonate-rich components which yielded two main groups. 1 st group consists of hematite, siderite, and ankerite minerals and comprises the ore while 2nd group is composed of calcite and serpentine minerals and comprises serpantinized lithologies. Each group displays a positive correlation internally while both groups show a negative correlation with respect to each other. Testing of some other component variations reveals once more the presence of two main groups. 1 st group consists of magnetite + hematite and ankerite + siderite while 2nd group is composed of calcite + dolomite and serpentine mineral variations. Evaluation of these groups yields the results similar to the previous one. The only difference is the accompaniment of dolomite occurrences.

## XRD studies on chemically analyzed samples

Minerals found with XRD studies performed on a number of 13 source and country rock and 12 chemically analyzed ore samples and the general petrographie features determined by microscope are described in Doğan(1996).

Component percents of 13 source and country rock samples were determined and correlation coefficients of all component pairs were computed. Moreover, correlation coefficients of some variations of components were also found. Examination of Table 7 reveals the presence of three groups. 1 st group consists of serpentine + olivine and magnetite minerals, 2nd group consists of only plagioclase, and 3rd group is composed of-tiastingsite + tremolite + pyroxene minerals. In the first group, there is a positive correlation with r = +0.94 among serpentine + olivine and magnetite minerals yielding an information in origin. 2nd group negatively correlates with 1 st group while 3rd group with 2nd and-1 st groups.

Calculation of correlation coefficients of all component and component variation pairs of 6 peridotite samples out of 13 source and country rock samples yields that serpentine, magnetite, and olivine minerals form one group and hastingsite, tremolite, chlorite, and pyroxene form another group. In general, there is a negative correlation between the two groups. Testing of some component variations indicates the presence of two main groups. 1st group consists of serpentine + olivine and magnetite minerals and yields a high positive correlation with r = +0.94. 2nd group is composed of hastingsite + tremolite + pyroxene minerals. This group negatively correlates with the first group with r = -0.98.

Calculation of correlation coefficients of all component and component variation pairs of 4 pyroxenite and 2 gabbro samples out of 13 source rock samples yields that hastingsite, tremolite, chlorite, and spinel comprise the first group while pyroxene comprises the second group and plagioclase makes up the third group. Minerals of first group are positively correlated with each other. Correlation coefficient of r = +0.99 between hastingsite and tremolite is significant. 2nd group negatively correlates with 1st group while 3rd group with 1st and 2nd groups. Testing of some component variations indicates the presence of two groups. 1 st group consists of hastingsite + tremolite + pyroxene minerals while 2nd group consists of only plagioclase mineral.

Table 7- Correlation coefficients of component pairs for source and country rocks [serpentine + olivine (Se-Ol), hastingsite + tremolite + pyroxene (Amp-pyx), plagioclase and magnetite component variations].

| | Se-Ol | Amp-Pyx | Plg | Mgn |
|---|---|---|---|---|
| Se-Ol | 1.00 | | | |
| Amp-Pr | -0.82 | 1.00 | | |
| Plg | -0.39 | -0.18 | 1.00 | |
| Mgn | 0.94 | -0.77 | -0.43 | 1.00 |

There is a significant negative correlation between the two groups with r = -0.98.

Furthermore, component percents together with correlation coefficients of component and component variables of chemically analyzed 12 ore samples were calculated that yielded the presence of two main groups. 1 st group consists of serpentine, chlorite, talc, siderite, ankerite, and hematite minerals while 2nd group is composed of quartz, calcite, magnetite, and pyroxene minerals. 1 st group minerals are positively correlated with each other while minerals of 2nd group are partly positively and negatively correlated. Therefore, there seems to be some difficulties in reevaluation of 2nd group minerals and in their grouping. However, testing of some component variables could be beneficial. Testing of magnetite + hematite, magnetite + hematite, and siderite + ankerite associations yields the 4th group. 1 st group has almost the same assemblage with the former first group. Serpentine, chlorite, talc, siderite + ankerite minerals comprise this group. This group is the indicative of vein mineralizations within hydrothermally altered country rocks. 2nd group is composed of quartz and calcite. These minerals indicate gangue minerals associated with vein mineralizations. 1st and 2nd groups are the indicative of ore veinlets. 3rd group is composed of only magnetite + hematite mineral assemblage and indicates the change of magnetites to hematite. 4th group is made of pyroxene mineral. These 4 groups are negatively correlated with each other. Negative correlation between 1 st and 2nd groups reflects the presence of gangue and vein type ore formation while negative correlation between 3rd and 1 st groups may probably indicate that ore minerals comprising the 1st group are derived from magnetite.

### Results of XRD studies

Vertical distribution of non-mineralized country rock samples from the Kes-2 well indicates the presence* of alternation of plagiocfase, pyroxene, and hastingsite (plus tremolite) while the mineralized parts reveal the association of clay, quartz, dolomite, ankerite, siderite, and magnetite (Fig. 7).

High positive correlation observed between hastingsite and tremolite minerals in non-mineralized parts of the same well indicates that most of hastingsites change to tremolite. However, negative correlation and inconsistency detected between pyroxene and tremolites hinder the searching of tremolite source in pyroxenes. In this respect, the relation of pyroxene hastingsite tremolite and changing of primary hastingsites to tremolite may be considered.

High negative correlation (r = -0.97) among plagioclase, pyroxene, and hastingsite + tremolite + pyroxene observed in non-mineralized part of the well yields the presence of a sequential association among plagioclase, pyroxene, and hastingsite minerals. In this case, it is believed that geostatistical expressions of cumulate textures of ultramafic cumulates are generally approached in accordance with negative correlation criteria.

In ore- and carbonate-dominated components of Kes-2 well, two different groups with negative correlations are detected. One is composed of magnetite + hematite + and ankerite + siderite while 2nd group consists of calcite + dolomite and serpentine minerals and their varieties which indicating that serpentinization accompanies and/or associated with the ore formation.

In addition to ore samples, Cluster Analyses of chemically analyzed peridotite samples of source and country rocks yield the presence of two groups, one is composed of serpentine + olivine and magnetite while the second consists of hastingsite + tremolite + pyroxene. In pyroxenite and gabbro samples, hastingsite + tremolite + pyroxene minerals comprise the first group while plagioclase comprises the second group. There is a negative correlation among these groups. In this case, it is thought that geostatistical expression of cumulate textures is approached with the correlation relation among mineral associations of each rock group.

Studies conducted on currently exploited massive ore samples indicate that 1st and 2nd groups are made up with serpentine, chlorite, talc, siderite + ankerite, and quartz and calcite minerals. These groups corres-

pond to ore-vein stage accompanied by hydrothermally altered gangue minerals in the country rock. 3rd group consists of hematitized magnetite while 4th group consists of pyroxene. Negative correlation between these 4 groups is distinctive.

Considering all the synthesis mentioned above, negative correlation between pyroxene observed in the ore samples and other 3 groups may indicate that minerals comprising the source of other groups should have been derived from plagioclase in pyroxenite and gabbro and from divine in peridotite. Since derivation of iron mineral from plagioclase is not possible, the source of this group seems to be olivine.

## RESULTS

1- Sediments of syntectonic basin that was developed under the control of ophiolitic rocks lying above the Paleozoic-Mesozoic basement of the Kırşehir Massive is characterized by a volcanosedimentary sequence consisting of sedimentary and volcanic rocks of upper Cretaceous Kasımağa formation that is laterally and vertically transitional with an ophiolite complex composing of ultramafic-mafic rocks together with crystallized limestone blocks. All these lithologies are intruded by Çelebi and Kesikköprü granitoids of Maastrichtian to Paleocene age. Typical skarn occurrences are observed along the contacts between granitic rocks and limestones while "skarn-like" and "fels-like" occurrences are detected far from granitic rocks and particularly within the mafic rocks. All these units are unconformably covered with post-tectonic basin sediments of Eocene Çayraz formation, Miocene-Pliocene (?) İncik formation, volcanic rocks, and Pliocene-Quaternary Kızılırmak formation.

2- As a result of petrographic and XRD studies, rocks associated with mineralization are divided into two parts, one is ultramafic rocks consisting of peridotite, pyroxenite, and serpentinites and the second is mafic rocks consisting of gabbro and diabase. Petrologic examination of core samples taken from the wells drilled in the Kesikköprü iron deposit reveals a stratigraphy, to a depth of 175 m, consisting of, from top to bottom, mafic rocks and hydrothermally altered mafic and ultramafic rocks. Alternated association between particularly olivine, pyroxene, and plagioclase minerals becomes distinctive in thin sections of hand specimens collected from the field and the area subjected to a detail ore geology study. Moreover, a banded texture is noticeable towards the surface. Petrographic studies on ultramafic and mafic rocks reveal the presence of ultramafic cumulates. However, since cumulate concept is a genetic description and it necessitates some petrologic studies, it should be avoided from using of such a concept. At the same time, cumulate texture should also be described in the field. Because the subject is related to ore geology, it is believed that a further study, on whether it is a typical ophiolitic sequence or it is crystallized as a result of insitu differentiation, is not needed.

3- Data from geochemical analyses on source rocks were plotted on a AFM diagram indicating that most of the samples are concentrated along FM axis. This yields a very close relation to the ophiolitic rocks of the Hatay region and partly to ophiolitic rocks of the Divriği area.

4- Findings on ore mineralogy of ore samples and ultramafic-mafic rocks are consistent. That is, granitic fluids may be directly associated with the ore formation. Ore is mainly composed of magnetite, lesser amounts of pyrite, chalcopyrite, chromite, siderite, ankerite, and trace amounts of pentlandite, gersdorffite, ilmenite, and sphene. Transformation products are frequently observed. Ore is accompanied by some silicate minerals, such as olivine, pyroxene, and tremolite, in addition, calcite and dolomite are also found along fracture and fissures.

Very fine grained, silicate mineral inclusion-bearing magnetites observed in ultramafic rocks have been intensely subjected to cataclysm due to tectonic settlement and early impacts of granitic rocks and they change to pure magnetites and are remobilized and recrystallized due to the circulations formed by hydrothermal convection cells in the country rocks which are heated by granitic rocks. This event may be observed within one same crystal size as changes to pseudo-zoned pure magnetites from crystal included parts towards the edges of crystal as well as zonings of centimeters in thickness. These indirect effects of granitic rocks may

redissolve such iron minerals during syngenetic and/or postgenetic processes and may also give rise to formation of siderite-ankerite veinlets traversing the structure.

Hydrothermal convection cell affecting the country rocks comprise the hydrothermal alteration models accompanied by "skarn-type minerals" and "fels-like textures". Tourmaline-rich isolated veinlets traverse the whole structure that are formed at later stages directly by the granitic fluids of different compositions following the same conduit. The whole structure in a wide region are also cut younger fluorite veins.

5- Absence of Zr, B, Sc, La, Ga, Y, Nb, Ce, and Nd elements in the ore samples indicates that granitic fluids are not effective for the ore formation.

Geochemical studies performed on the ore samples yield that source of iron element may be derived from ultramafic rocks. Ultramafic rocks being enriched in iron due to serpentinization are leached by indirect effects of granitic rocks, and thus country rocks become iron-poor and the iron expelled may form the mineral associations, hence the iron deposits, at suitable Eh and pH conditions (Fig. 9).

Therefore, as a result of serpentinization, expelling of iron element in ferromagnesian minerals of ultramafic rocks, such as olivine and partly pyroxene, is the primary source of iron. Their secondary enrichment by the granitic fluids indicates another important stage in the formation of Kesikköprü iron deposit.

## DISCUSSION-COMPARISON AND SUGGESTIONS

In the previous studies (Kraeff, 1962; Boroviczeny, 1964a, *b, c,* c, d, Sözen, 1970; Öztürk et al., 1983), Kesikköprü iron deposits was thought to be a skarn type deposit associated directly with granitic rocks. However, recent works on the formation of modeling of iron deposits (Ünlü, 1989; Ünlü and Stendal, 1986 a, *b;* 1989; Stendal and Ünlü, 1991; Ünlü et al., 1995) state that iron enrichments deriving from ophiolitic rocks due to indirect effects of granitic rocks. It is also suggested that ophiolitic rocks are the source of iron element in synsedimentary-volcanogene or exhalative-sedimentary deposits within the basins formed on the ophiolitic complex (Ünlü, 1983; Stendal et al., 1995; Çiftçi et al., 1996; Ünlü et al., 1996).

In the frame of this study, it is suggested that Kesikköprü iron deposit is a Divriği type deposit (Gümüş, 1979: pyro-mobile-metasomatic, Ünlü et al., 1995: metamorphic + hydrothermal alteration type), that is, iron is not derived from granitic rocks but formed by the enrichment resulting from dissolution of source rocks. The fact that country rocks are not mostly carbonaceous rocks restricts to use of the term of "skarn-type deposits". Therefore, in general, Kesikköprü iron deposits may be described as a deposit associated with "magmatism-metamorphism" processes (Guilbert and Park, 1986). However, although small limestone relicts observed as blocks within ultramafic and mafic rocks seem to be not directly affected from this process, considering the field observations and theoretic assumptions, it should not be precluded that such a process may facilitate formation of skam minerals and fels textures.

It seems inevitable that an investigations should be directed to discovering of new magnetite deposits in the lithologies belonging to ophiolitic melange around the Kesikköprü area, and then, studying the altered rocks by air-borne electric and magnetic methods while ore occurrences by means of air-borne magnetic method, and by justifying the data obtained with those from magnetic method performed in the field, target areas have to be selected and finally detailed geological studies should be carried out. It should be always considered that during these studies, new iron and manganese deposits could be discovered in volcanosedimentary sequences.

## ACKNOWLEDGEMENTS

This work comprises a part of first author's M. Sc. study conducted in the Department of Geological Engineering of the Ankara University under the guidance of

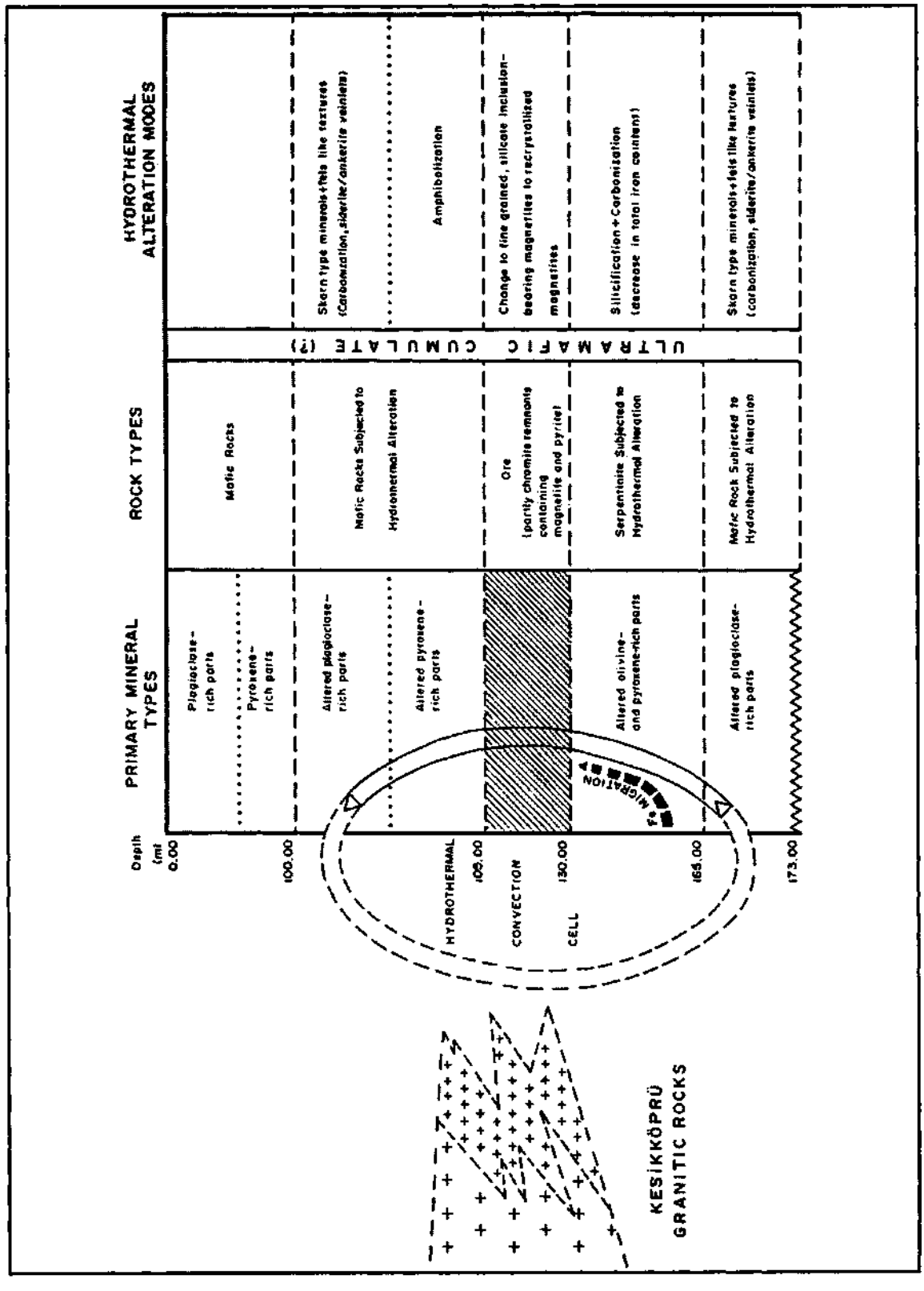


Fig. 9- Probable formation model of Kesikköprü iron deposit (figure is producted from the data of Kes-2 well. No scale).

second and third authors. Authors thank to Prof. Ayhan Erler, Dr. Ahmet Çağatay, Prof. Baki Varol, and Assoc. Prof. Okan Tekeli for their criticism on the manuscript. Appreciation is extended to General Directorate of MTA for the access of geochemical studies. Thin sections and duplicate samples of rocks are stored at the laboratories of Department of Geological Engineering of the Ankara University.

Manuscript received November 22, 1996

## REFERENCES

Akıman, O.; Erler, A.; Göncüoğlu, M.C.; Güleç, N.; Geven, A.; Türeli, T.K. and Kadıoğlu, Y.K., 1993, Geochemical characteristics of granitoids along the western margin of the Central Anatolian Crystalline Complex and their tectonic implications: Geological Journal, 28, 371 - 382.

Akyürek, B.; Bilginer, E.; Akbaş, B.; Hepşen, N.; Pehlivan, S.; Sunu, O.; Dağer, Z.; Çatal, E.; Sözeri, B.; Yıldırım, H. and Hakyemez, Y., 1984, Ankara - Elmadağ - Kalecik dolayının temel jeoloji özellikleri: Jeo. Müh., 20, 5-19, Ankara.

Atabey, E.; Tarhan, N.; Akarsu, B. and Taşkıran, A., 1987, Şereflikoçhisar, Şanlı (Ankara) - Acıpınar (Niğde) yöresinin jeolojisi: MTA Derleme Rep., 8155, (unpublished), Ankara.

Ataman, G.,1972, Ankara'nın güneydoğusundaki granit-granodiyoritik kütlelerden Cefalık dağ'ın radyometrik yaşı hakkında ön çalışma: H. Ü. Yerbilimleri Derg., 2/1, 44 - 49, Ankara.

Ayan, M., 1963, Contribution a l'etude Petrographique et geologique de la region situee au Nord-Est de Kaman (Turquie): MTA Bull., 115, 332 s.

Bailey, E. B. and Mc Callien, W.J., 1950, Ankara Melanjı ve Anadolu Şariyajı: MTA Bull., 40,17 - 21, Ankara.

Bayhan, H., 1984, Kesikköprü skarn kuşağının (Bala - Ankara) mineralojisi ve petrojenezi: H. Ü. Yerbilimleri Derg., 11 ,45-57, Ankara.

Bayhan, H., 1986, İç Anadolu granitoyid kuşağındaki Çelebi Sokulumu'nun jeokimyası ve kökensel yorumu: Jeo. Muh., 29, 27 - 36, Ankara.

Bilgin, Z.R.; Akarsu, B.; Erbaş, A.; Elibol, E.; Yaşar, T.; Esentürk, K.; Güner, E. and Kara, H., 1986, Kırıkkale - Kesikköprü - Çiçekdağı alanının jeolojisi: MTA Gen. Müd., Derleme Rep., 7876, (unpublished), Ankara.

Boroviczeny, F., 1964a, 200/240 no'lı ruhsat sahasının Kesikköprü yakınındaki demir yatağı hakkındaki rapor: MTA Rep., 3481, (unpublished) Ankara.

———, 19646, 200/212 no'lı ruhsat sahasında yapılan jeolojik etütler hakkında sunulan rapor. MTA Rep., 3570, (unpublished), Ankara.

———, 1964c, Kesikköprü yakınındaki 200/240 no'lı ruhsat sahasında yapılan jeolojik etütler hakkında rapor: MTA Rep., 3591, (unpublished), Ankara.

———, 1964d, 200/248 no'lı ruhsat sahasında yapılan jeolojik etütler hakkında sunulan rapor: MTA Rep. 3584, (unpublished), Ankara.

Boudier, F. and Coleman, R.G., 1981, Cross section through the peridotite in the Samail Ophiolite, Southeastern Oman Mountains: Journal of Geophys. Res., 86, B4, 2573 - 2593, Londra.

Brennich, G., 1960, Çelebi - Kesikköprü - Hirfanlı Bölgesinde manyetit zuhurları hakkında rapor: MTA Rep., 2755, (unpublished) Ankara.

Çapan, U.Z. and Buket, E., 1975, Aktepe - Gökdere bölgesinin jeolojisi ve ofiyolitli melanj: TJK Bült., 18, 11 -16, Ankara.

Çiftçi, D., Ünlü, T. and Sayılı, I.S., 1996, Otlukilise (Gürün-Sivas) demir yatağının kökenine bir yaklaşım: MTA Bull., 118, 65-92, Ankara.

Doğan, B., 1996, Kesikköprü Demir Yatağı'nın (Bala - Ankara) maden jeolojisinin incelenmesi: A.Ü.F.F. Jeo. Müh. Bölümü, Yüksek Lisans Tezi, 258 p. (unpublished), Ankara.

Egeran, N. and Lahn, E., 1951, Note on the tectonic position of the northern and central Anatolia: MTA Bull., 41,23-27, Ankara.

Erkan, Y., 1981, Orta Anadolu Masifinin metamorfizması üzerinde yapılmış çalışmalarda varılan sonuçlar: İç Anadolu'nun Jeolojisi Simpozyumu TJK Bull., 9-11, Ankara

———and Ataman, G., 1981, Orta Anadolu Masifinin (Kırşehir Yöresi) metamorfizma yaşı üzerinde K/Ar yöntemi ile bir inceleme: TJK 35. Kurultay, Bildiri Özetleri, 33, Ankara.

Erler, A; Akıman, O.; Unan, C.; Dalkılıç, F.; Dalkılıç, B.; Geven, A. and Önen, A.P., 1989, Kaman (Kırşehir) ve Yozgat yörelerinde Kırşehir Masifi magmatik kayaçlarının petrolojisi ve jeokimyasi: TÜBİTAK Proje No: TBAG 677,119 p., Ankara.

;———;———;———;———;———and ———, 1991, Kaman (Kırşehir) ve Yozgat yörelerinde Kırşehir Masifi magmatik kayaçlarının petrolojisi ve jeokimyası: TÜBİTAK, Doğa, 15, 76-100, Ankara.

———and Bayhan, H., 1995, Orta Anadolu granitoidlerinin genel değerlendirilmesi ve sorunları: Yerbilimleri, 17, 49-67, Ankara.

Göncüoğlu, M.C., 1977, Geologie des westlichen Niğde Massivs: Bonn Üniv. Doktora Tezi, 181 p. (unpublished), Bonn.

Guilbert, J. M. and Park, C.F., 1986, Skarn Deposits: The Geology of Ore Deposits. 436 - 451, A.B.D.

Güleç, N., 1994, Rb - Sr Isotope data from the Ağaçören Granitoid (east of Tuz Gölü). Geochronological and genetical implications: J. of Earth Sciences, 3, 39 - 43, TÜBİTAK, Ankara.

Gümüş, A., 1979, Nouvelles observations sur la genese du gisement de Fer de Divriği (Sivas, Turguie): Verh. Geol. B-A, 3, 347-355.

Kara, H. and Dönmez, M., 1990,1/100.000 ölçekli açınsama nitelikli Türkiye jeoloji haritaları serisi: Kırşehir - G17 paftası No: 34, MTA Bull., Ankara.

Ketin, İ., 1955, Yozgat Bölgesi'nin jeolojisi ve Orta Anadolu Masifi'nin tektonik konumu: TJK Bull., 6,1 - 40, Ankara.

Ketin, İ,.1963, 1/500.000 ölçekli Türkiye Jeoloji Haritası Kayseri Paftası izahnamesi: MTA Bull., Ankara.

Kraeff, A., 1962, Kesikköprü konsesyonu: MTA Gen. Müd., Derleme Rep., 3349, (unpublished) Ankara.

Norman, T., 1972, Ankara-Yahşihan bölgesinde Üst Kretase-Alt Tersiyer istifinin stratigrafisi: TJK Bull., 15/2,180-276, Ankara.

Önen, P. and Unan, C., 1988, Kaman (Kırşehir) kuzey doğusunda bulunan gabroların mineralojisi, petrografisi ye jeokimyası: TJK Bull., 31 , 23 - 28, Ankara.

Öztürk, M., 1981, Ankara-Keskin-Çelebi; Kırşehir-Kaman; Nevşehir-Hacıbektaş yörelerindeki demir zuhurlarının jeoloji raporu: MTA Gen. Müd., Rep., 7158, (unpublished), Ankara.

Öztürk, K. and Öztürk, M., 1983, Ankara-Bala-Yukarıtepeköy-Kartalkaya demir cevherleşmesi Jeoloji Etüt ve Arama Raporu, MTA Gen. Müd., Rep. 7357, (unpublished), Ankara.

———, Kurt. M.; Öztürk, M. and Sarı, İ., 1983, Ankara-Bala-Kesikköprü, Madentepe, Büyükocak, Çataldere, Camiisagir demir yatakları jeoloji ve rezerv raporu: Cilt 1, 2, 3, MTA Gen. Mud. Rep. 7355, (unpublished), Ankara.

Schmidt, C.G., 1960, Mem. 365-367 no'lı ruhsat sahalarının nihai terk raporu: Petrol İşleri Gen. Müd., (unpublished), Ankara.

Seymen.İ.,1982, Kaman dolayında Kırşehir Masifinin Jeolojisi: ITU Maden Fakültesi Doçentlik Tezi, 164 p., Istanbul.

Sözen, A., 1970, Kesikköprü, Madentepe manyetit zuhur hakkında rapor: MTA Gen. Mud. Rep. 4212, (unpubhished), Ankara.

Stendal, H. and Ünlü, T., 1991, Rock geochemistry of an iron ore field in the Divriği region, Central Anatolia, Turkey. A new exploration model for iron ores in Turkey: Journal of Geochemical Exploration, 40, 281 - 289, Amsterdam.

———,———and Konnerup-Madsen, J., 1995, Geological setting of iron deposits of Hekimhan Province, Malatya, Central Anatolia, Turkey: Trans. Instn Min. Metall. (Sect. B: Appl. earth sci.), 104,46 - 54, London.

Sungurlu, B., 1970, Kesikköprü-Çelebi-Hirfanlı Bölgesinin manyetit zuhurları hakkında (Yaz and Sözen) isimli rapordan Kesikköprü Ltd. Şirketine ait Ar: 200/248 ruhsat no'lı demir sahası için derlenen rapordur: MTA Gen. Mud. Rep. 4231, (unpublished) Ankara.

Tülümen, E., 1980, Akdağmadeni (Yozgat) yöresinde petrografik ve metalojenik incelemeler: KTÜ Doktora Tezi, 157 p., Trabzon.

Ünlü, T., 1983, Die Genese der Siderit-Lagerstatte Deveci in der Hekimhan-Provinz Malatya/Turkei und ihre wirtschaftliche Bewertung: Doktora çalışması, Berlin Teknik Üniversitesi, 84 p., Almanya.

———, 1989, Türkiye demir yatakları arama çalışmalarında 1. derecede ağırlıklı hedef saha seçimi ve maden jeolojisi araştırmaları ile ilgili proje teklifi: MTA Gen. Mud. Rep., 8593, 48p., (unpublished), Ankara.

———, Sayılı, I.S. and Çiftçi, D., 1996, An approach on genesis of Otlukilise iron deposit Gürün - Sivas, Middle Anatolia - Turkey: UNESCO, IGCP, Project No 356, Alpine metallogeny and plate tectonics in the Carpatho - Balkanides, v. 2,15-22, Sofya, Bulgaristan.

———and Stendal, H., 1986a, Divriği Bölgesi demir yataklarının element korelasyonu ve jeokimyası (Orta Anadolu - Türkiye): Jeo. Müh., 28, 5-19, Ankara.

Ünlü, T. and Stendal, H., 1986b, Jeokimya verilerinin çok değişkenli jeoistatistik analizlerle değerlendirilmesine bir örnek. Divriği bölgesi demir yatakları, Orta Anadolu: MTA Bull., 109, 127-140, Ankara.

———and———, 1989, Divriği Bölgesi demir cevheri yataklarının nadir toprak element (REE) jeokimyası. Orta Anadolu, Türkiye: TJK Bull., 32 (1- 2), 21-38 Ankara.

———,———, Makovisky, E. and Sayılı, I. S., 1995, Divriği (Sivas) demir yatağının kökeni, Orta Anadolu, Turkiye - Bir cevher mikroskobisi çalışması: MTA Bull., 117,17 - 28, Ankara.

Yaz, N. and Sözen, A., 1965, Kesikköprü Madencilik Ltd. Şirketi Kesikköprü Demir Ruhsat sahaları hakkında rapor: MTA Rep., 3810, (unpublished), Ankara.

———and———, 1967, Kesikköprü - Çelebi - Hirfanlı bölgesinin manyetit + hematit zuhurları hakkında rapor: MTA Rep., 4440, (unpublished), Ankara.

Wondemagegnehu, T. W., 1990, Mineralogy, chemistry and physical properties of the magnetite ore deposits around Kesikköprü village and the surrounding areas: ODTÜ Yüksek Lisans Tezi, 128 s., Ankara.

PLATES

**PLATE-I**

Fig. 1 - Pyroxenes (grained parts at the top) of banded texture and plagioclases (light colored part at the bottom) within the gabbro. XPL. Magnification x16 .

Fig. 2- Carbonated (subjected to hydrothermal alteration) magnetite crystals (small black grains on the left center) oriented in the serpentinite. XPL. Magnification x16 .

Fig. 3- Magnetite veinlets (black) and chromite grains (four black grains on the right bottom) within serpentinized ultramafic rock (dunite). XPL. Magnification x16 .

Fig. 4- Magnetite (black) and silicate occurrences (light gray) within magnetite in carbonated serpentinite (subjected to hydrothermal alteration). XPL Magnification x16 .

Fig. 5- Chromite (black margin at the right bottom) in serpentinite (dark gray at left) - cataclastic textured chromite-magnetite assemblage associated with spinel (light gray spots) and magnetite (white) transitions. In oil. Magnification x200.

Fig. 6- Deformed orthopyroxene (gray) and magnetite occurrences (white) along the cleavages. In oil. Magnification x200.

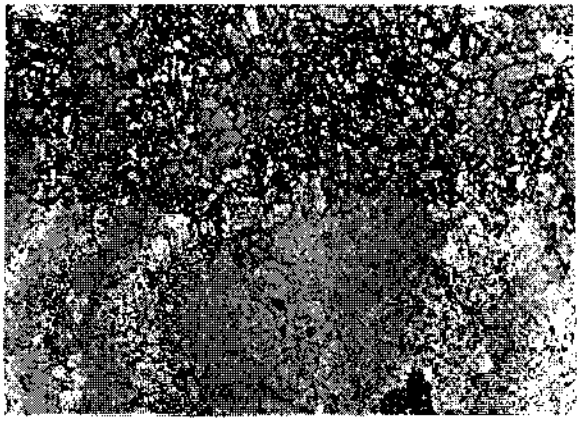

1

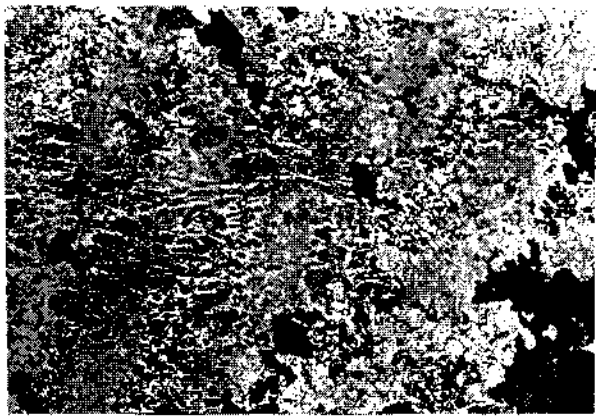

2

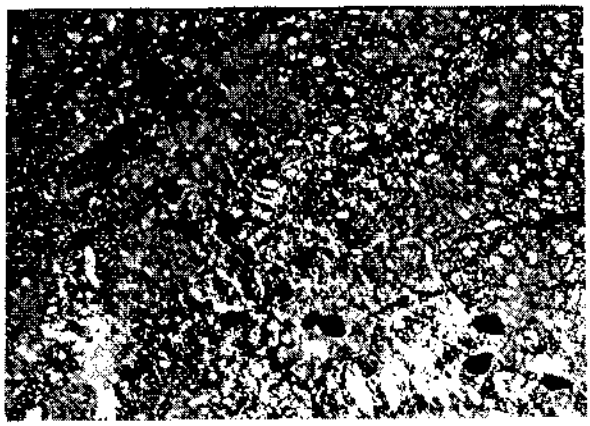

3

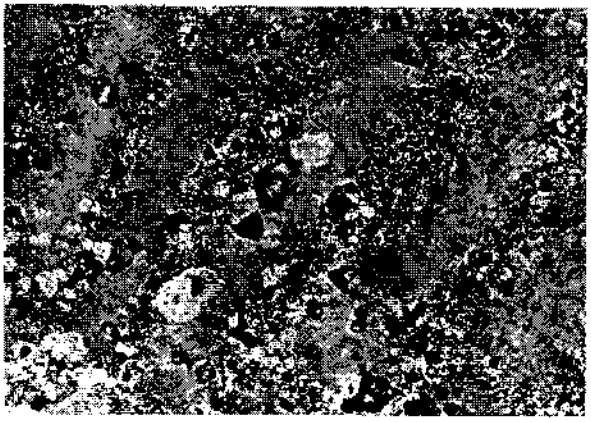

4

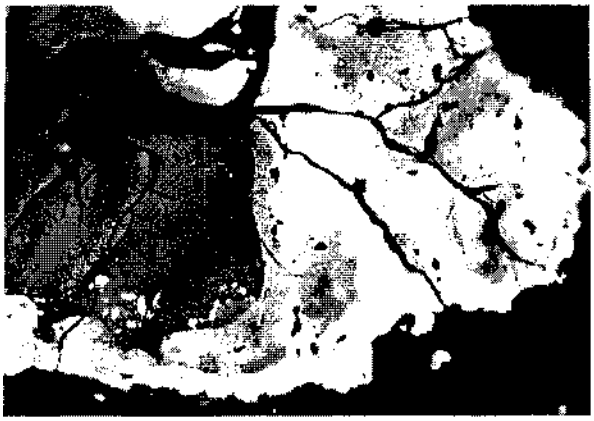

5

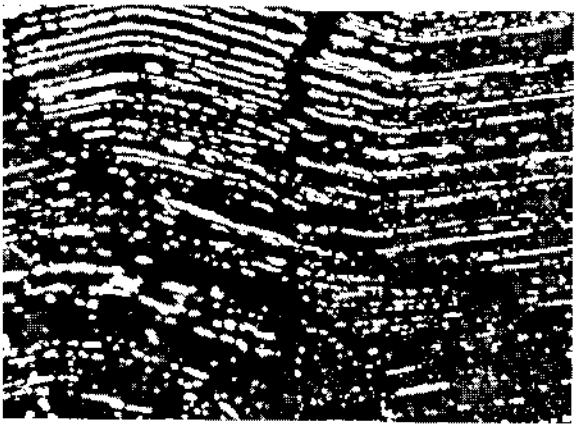

6

**PLATE-II**

Fig. 1- Magnetite (gray) and pentlandite (dirty white, anhedral at the left center) growths and a gersdorffite grain (white, subhedral at the center) in serpentinites (black). In oil. Magnification x200.

Fig. 2- Hercynite occurrences (gray) along cleavage plains of orthopyroxene (dark gray). In oil. Magnification x200.

Fig. 3- Silicate inclusion-bearing (small black spots) magnetite occurrences (gray) associated with siderite-ankerite type carbonates (black coarse grains) along fracture and spaces. In oil. Magnification x200.

Fig. 4- Cataclastic magnetite occurrences (gray) transforming to martite along the edges. In oil. Magnification x200.

Fig. 5- Tremolite, actinolite, and chlorite (horn-shaped dark gray part at the center) inclusions-bearing chalcopyrite occurrences (gray) locally transformed to bornite (dark gray cloudy appearance at the left center) in siderite-ankerite (black). In oil. Magnification x200.

Fig. 6- Chromite and chrome spinel (gray central parts of the same crystal) occurrences in calcite-dolomite (cloudy gray background) transformed to magnetite (the most outer light gray zone of drop-shaped crystals) along the margins. In oil. Magnification x200.

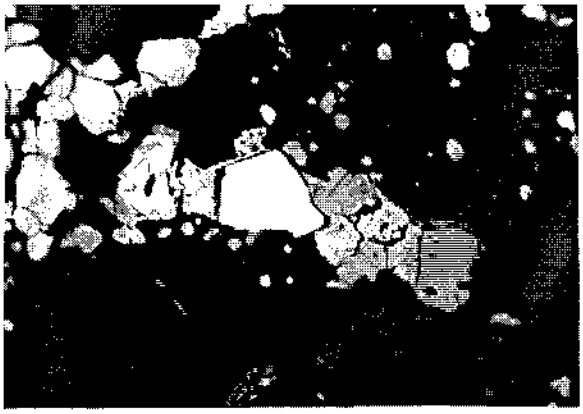

1

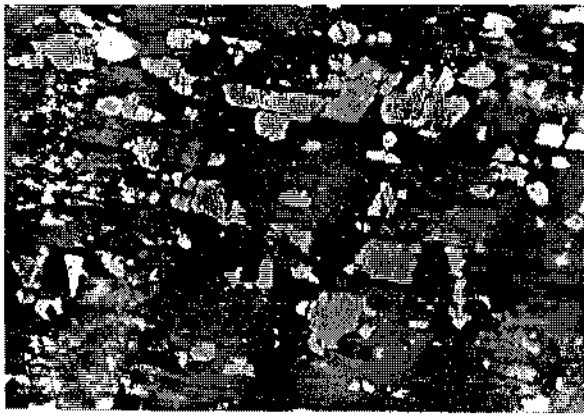

2

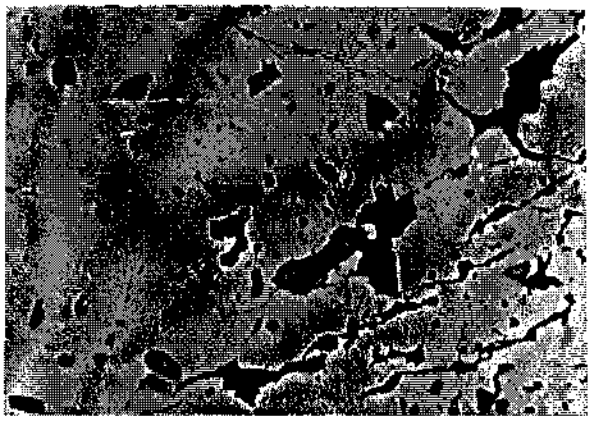

3

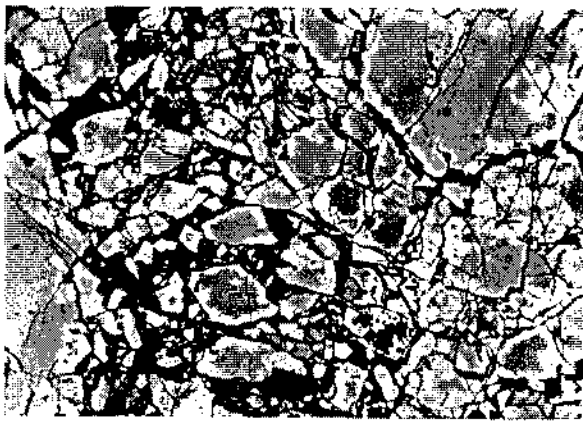

4

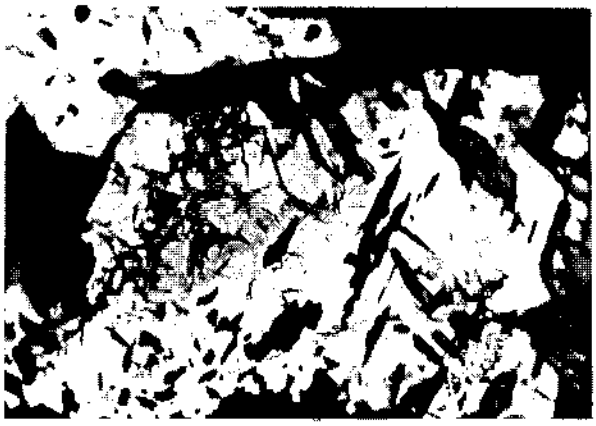

5

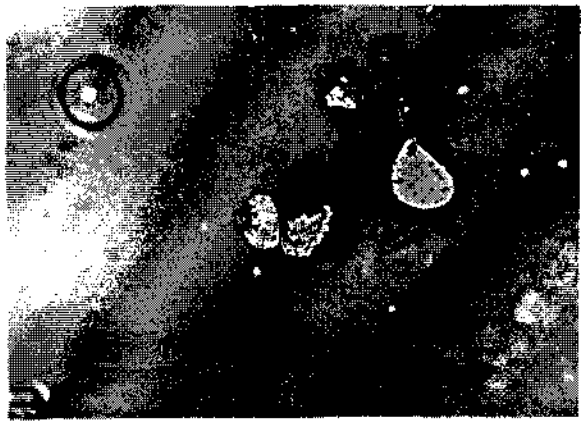

6